Technische Universität München

TUM School of Medicine and Health

Retrogenic color-barcoding as a novel method to investigate lymphocyte differentiation and migration on single-cell level

Ludwig Otto Pachmayr

Vollständiger Abdruck der von der TUM School of Medicine and Health zur Erlangung eines

Doktors der Medizinischen Wissenschaft (Dr. med. sci.)

genehmigten Dissertation.

Vorsitz: Prof. Dr. Dirk H. Busch

Prüfende der Dissertation:

1. Priv.-Doz. Dr. Veit Buchholz
2. Prof. Dr. Jürgen Ruland
3. Prof. Dr. Thomas Brocker

Die Dissertation wurde am 21.02.2024 bei der Technischen Universität München eingereicht und durch die TUM School of Medicine and Health am 05.06.2024 angenommen.

Parts of this thesis have previously been published:

Grassmann S[*], **Pachmayr LO**[*], Leube J, Mihatsch L, Andrä I, Flommersfeld S, Oduro J, Cicin-Sain L, Schiemann M, Flossdorf M, Buchholz VR. Distinct Surface Expression of Activating Receptor Ly49H Drives Differential Expansion of NK Cell Clones upon Murine Cytomegalovirus Infection. *Immunity* (2019)

Grassmann S[*], Mihatsch L[*], Mir J, Kazeroonian A, Rahimi R, Flommersfeld S, Schober K, Hensel I, Leube J, **Pachmayr LO**, Kretschmer L, Zhang Q, Jolly A, Chaudhry MZ, Schiemann M, Cicin-Sain L, Höfer T, Busch DH, Flossdorf M, Buchholz VR. Early emergence of T central memory precursors programs clonal dominance during chronic viral infection. *Nature Immunology* (2020)

Flommersfeld S[*], Böttcher JP[*], Ersching J, Flossdorf M, Meiser P, **Pachmayr LO**, Leube J, Hensel I, Jarosch S, Zhang Q, Chaudhry MZ, Andrä I, Schiemann M, Busch DH, Cicin-Sain L, Sun JC, Gasteiger G, Victora GD, Höfer T, Buchholz VR[†], Grassmann S[†]. Fate mapping of single NK cells identifies a type 1 innate lymphoid-like lineage that bridges innate and adaptive recognition of viral infection. *Immunity* (2021)

Purcarea A*, Jarosch S*, Barton J, Grassmann S, **Pachmayr LO**, D'Ippolito E, Hammel M, Hochholzer A, Wagner KI, van den Berg JH, Buchholz VR, Haanen JBAG, Busch DH[†], Schober K[†]. Signatures of recent activation identify a circulating T cell compartment containing tumor-specific antigen receptors with high avidity. *Science Immunology* (2022)

Pachmayr LO*, Muehlbauer A*, Flommersfeld S, Graml F, Hoenninger J, Von Baumgarten L, Buchholz VR[†], Grassmann S[†]. Unbiased chemokine receptor screening reveals similar efficacy of lymph node- and tumor-targeted T cell immunotherapy. *Cancer Immunology Immunotherapy* (2023)

---

* These authors contributed equally, † These authors jointly supervised this work

Table of Contents

Index of Figures

Abbreviations

ACT	Ammonium chloride-Tris
BHI	Brain heart infusion
CCR	CC chemokine receptor
CD	Cluster of differentiation
CFU	Colony forming unit
CLP	Common lymphoid progenitor
CR	Chemokine receptor
CXCR	CXC chemokine receptor
DC	Dendritic cell
DMEM	Dulbecco's modified eagle medium
EDTA	Ethylenediaminetetraacetic acid
EMA	Ethidium monoazide bromide
FACS	Fluorescence activated cell sorting
FCS	Fetal calf serum
Flt3	FMS-like tyrosine kinase 3
FP	Fluorophore
GFP	Green fluorescent protein
GM-CSF	Granulocyte-macrophage colony-stimulating factor
Gy	Gray
hIL-2	Human Interleukin 2
HSC	Hematopoietic stem cell
HSCT	Hematopoietic stem cell transplantation
IL	Interleukin
ILC	Innate lymphoid cell
i.p.	Intraperitoneal
i.v.	Intravenous
LTi	Lymphoid tissue inducer
MCMV	Murine cytomegalovirus
MDCS	Myeloid-derived suppressor cells

MHC	Mature histocompatibility complex
mRNA	Messenger RNA
mSCF	Murine stem cell factor
NFIL3	Nuclear factor, interleukin 3 regulated
NK	Natural killer
NKP	Natural killer progenitor
OD	Optical densitiy
OVA	Ovalbumin
PBS	Phosphate buffered saline
PD-1	Programmed cell death protein 1
PI	Propidium iodide
p.i.	post injectionem
PLAT-E	Platinum-E
RT	Room temperature
s.c.	Subcutaneous
scRNAseq	Single cell RNA sequencing
TCR	T cell receptor
Treg	Regulatory T cell
XCR	C chemokine receptor

1 Introduction

1.1 Immunology research as the basis for successful therapies

Immunotherapy marks a milestone in the history of medical research. By supporting the immune system, restricting or replacing it, mankind achieved eradication of certain infectious diseases (Jenner, 1801, Pasteur, 1881a, Pasteur, 1881b, Hilleman et al., 1967), improved the durability of foreign organ transplants (Battaglia et al., 2005, Araki et al., 2009) and devised new approaches to fight malignant tumors (Hodi et al., 2010, Neelapu et al., 2017, Maude et al., 2018). Recently, the emergence of a global pandemic caused by a coronavirus has been answered in an unparalleled fashion by the rapid development of safe and efficient vaccines (Polack et al., 2020, Cohen et al., 2021, Dai and Gao, 2021, Wu et al., 2023). The foundation for this progress was laid by basic immunological research. Growing comprehension of signaling pathways, molecular processes, cell types and subsets, and their genetic and epigenetic regulation enabled the development of more effective and more specific therapies.

1.2 Differentiation, proliferation and maturation of immune cells

Vertebrate immune cells comprise a variety of different cell types that all originate from a common progenitor, the hematopoietic stem cell (HSC) (Becker et al., 1963, Williams, 1994). Further development in the bone marrow niche leads to common myeloid, as well as lymphoid progenitor cells. These common precursors give rise to mature immune cells like Dendritic cells (DCs), granulocytes, monocytes and macrophages, Natural killer (NK) as well as B and T cells (Jagannathan-Bogdan and Zon, 2013, De Kleer et al., 2014). T cells and NK cells have been intensively studied in the context of viral infection and cancer. On the one hand, a malfunction of these cells can lead to severe immunodeficiency and susceptibility to infectious and malignant diseases (Glanzmann and Riniker, 1950, Biron et al., 1989). On the other hand, recent studies have shown their intriguing therapeutic potential in the context of adoptive cell transfer, targeting cancer and HSCT-derived chronic viral infection (Rosenberg et al., 2011, Heslop et al., 2010).

Both T and NK cells are generated from Common lymphoid progenitors (CLPs) (Kondo et al., 1997). When entering the thymus, T cell precursors further differentiate along the T cell lineage. This process is accurately controlled in certain thymical areas, namely the subcapsular zone,

cortex, corticomedullar junction, as well as medulla. Characterized by the expression and restriction of surface molecules like CD4, CD8, CD25, CD44, and CD117, as well as T cell receptor (TCR) signaling and somatic recombination via *Rag*, early thymic progenitors eventually develop into mature naïve T cells (Koch and Radtke, 2011). On the other hand, differentiation of NK precursors (NKPs) is controlled by the transcription factor *Nfil3*, directly regulating gene expression of *Eomes* and *Id2* in bone marrow CLPs (Male et al., 2014). Further maturation is then driven by surface molecule expression of inhibitory and activating receptors (Kim et al., 2002). Interaction between germline-encoded NK cell receptors and MHC class I molecules helps to further acquire functional competence, a process termed 'licensing' (Kim et al., 2005).

Homeostasis of these mature immune cells is furthermore controlled by stimulation of cytokine receptors, as well as their specific T and NK cell receptors. Somatic recombination and avidity maturation of the T cell receptor result in a highly specific recognition of non-self antigens, as one optimized receptor binds to a peptide presented on MHC class I or II (Jameson, 2002). This acquired specificity represents a hallmark of adaptive immunity. In contrast, NK cells express a combination of germline-encoded receptors that recognize dysregulated-self signals, e.g. downregulation of MHC class I or upregulation of stress ligands (Sun and Lanier, 2011). More recently however, it has been shown that some of these NK cell receptors also recognize molecules encoded by certain viruses, thereby, acting as specific non-self receptors as well (Dokun et al., 2001, Sun et al., 2009). These findings implicated certain adaptive features of NK cell biology.

Taken together, immune cell differentiation and maturation are delicate biological mechanisms. Regarding T and NK cells as fundamental cellular agents of an individual's immune system, basic immunological research revealed apparent differences concerning their development and functionality. Respectively to recent work however, further investigation of NK cell mechanisms on a clonal level may lead to novel aspects concerning their expansion capacity, functional receptor management, and more parallels, as well as differences to T cell behaviour. Since NK cells do not have a unique TCR that could serve as label of shared clonal origin, one must apply other approaches to monitor clonal dynamics within NK cell responses to viral infection.

1.3 In vivo fate mapping of single immune cells to study immune cell differentiation and proliferation

Tracing immune responses emerging from individual T cells and investigating their offsprings' proliferative expansion and phenotypic differentiation in vivo has emerged as a valuable asset in immunological research (Buchholz et al., 2016). When adoptively transferring immune cells into an experimental animal, retrieving and distinguishing the offspring of these cells is pivotal to address questions like lineage relationships, cell fate or proliferative capacity. For a long time, these questions were addressed by adoptive transfer of lymphocyte populations. However, this assessment of average population behavior only allowed for limited deduction of the actual clonal properties emerging from an individual responding lymphocyte. While for T cells, responding to an infection or vaccination, the sequence of their TCR is often considered as a marker for their shared clonal origin, this assumption must be made with some caution, due to the proliferative expansion of TCR-identical naïve T cells already before infection. Thus, to monitor true single-cell origin among T cell and other lymphocytes, in the past years various approaches have been developed.

Cellular barcoding refers to a technique that tags individual progenitor cells with a molecular DNA barcode that can be analyzed by microarray hybridization (Schepers et al., 2008). In this context, the barcode represents a distinct non-coding DNA sequence. Combining the barcode with a DNA sequence encoding for a specific fluorescent protein and implementing both in a retroviral vector allows for transduction and barcoding of target cells. After adoptive transfer, proliferated and differentiated barcoded cells can be isolated via flow cytometric sorting and barcode analysis can be performed via DNA hybridization on microarray slides (Schepers et al., 2008). Analyzing the cell populations using next-generation sequencing even allows the investigator to quantify the prevalence of a barcode within a given cell population (Gerlach et al., 2013, Naik et al., 2013).

However, since cellular barcoding requires DNA extraction accompanied by cell lysis, detection of genetic barcodes is incompatible with subsequent functional analyses. This instead requires clonal labels that can be "read" on live cells, which can be achieved e.g. by use of congenic markers combined with flow cytometry and adoptive single-cell transfer. Congenic mice share the same genome in comparison to wildtype C57BL/6 mice, apart from only one specific gene locus. The most common congenic mouse strain is a strain where the protein tyrosine phosphatase CD45, expressed on all nucleated haematopoietic cells including leukocytes, is mutated (Kishihara et al., 1993). Mice of this strain express the functionally

identical isoform CD45.1, whereas wildtype C57BL/6 express the allele CD45.2 (Shen et al., 1985). As a surface protein, CD45 expression can easily be detected via flow cytometry. CD45.1 leukocytes that are transferred into wild type CD45.2 recipients can be differentiated from host cells and therefore either be phenotypically analyzed or sorted for further adoptive transfer. This trait allows to address single cell properties that require live cells such as the ability to reexpand upon exposure to secondary infection, a hallmark of immunological memory (Sallusto et al., 2004). Due to the codominant expression of both CD45 alleles upon adoptive transfer, two traceable clones can be discerned from CD45.2/.2 expressing host cells, namely homozygous CD45.1/.1 and heterozygous CD45.1/.2 cells. By using more than one congenic marker, the number of discernable clones or immune cell populations can be increased. Combining CD45 with CD90, which is another surface protein expressed on lymphoid and nervous tissue (Reif and Allen, 1964), enables transfer of up to 8 individual cells or lymphocyte populations into the same wild type recipient (Buchholz et al., 2013), thereby, increasing data output while reducing required numbers of recipients at the same time.

Single-cell fate mapping has led to intriguing insights into immune cell biology. A single antigen-specific progenitor T cell clone proved to be able to generate diverse offspring with a functional range of short-lived effector cells to long-lived effector cells (Stemberger et al., 2007). Furthermore, clonal analyses elucidated the striking variability of proliferative capacity, phenotypic differentiation and recall capacity within immune response emerging from TCR-identical T cells (Buchholz et al., 2013). However, since CD90 is not stably expressed in leukocytes other than T cells, application of the congenic matrix for other immune cell lineages is limited.

Consequently, future studies require novel technologies that combine the virtues of both genetic cellular barcoding and congenic markers. Enabling a swift and simple label introduction into new genetic backgrounds, which can be extended to a variety of immune cells is inevitable in order to extend the scope of single-cell fate mapping beyond T cell lineages.

1.4 Immune cell migration and its role in disease control

Besides controlled differentiation and maturation, localization of immune cells is crucial for immunity. Migratory patterns and positioning of immune cells are controlled by chemotactic cytokines called chemokines. Chemotaxis is exerted via binding of more than 40 various chemokines to 18 different signalling G-protein coupled chemokine receptors, as well as 4 –

so called – atypical, nonsignaling receptors (Griffith et al., 2014). T cell development is based on thymic interactions at multiple locations, orchestrated by CCL21, CCL25 and CXCL12 binding to CCR7, CCR9 and CXCR4, respectively, expressed on T cell progenitors (Love and Bhandoola, 2011). Homeostatic regulation of immune cell development in the bone marrow also depends largely on CXCL12/CXCR4 interactions, retaining HSC populations in their niches and promoting physiological immune cell differentiation (Peled et al., 1999, Ara et al., 2003, Mercier et al., 2011). Formation of secondary lymphoid organs relies on CXCL13-dependent clustering of LTi cells expressing its corresponding receptor CXCR5, as well as the CCL19/21-CCR7 axis (Luther et al., 2003, Ohl et al., 2003). Immune cell localization in peripheral tissues is controlled likewise. CX_3CR1 expression on blood monocytes can lead to development into tissue macrophages via CX_3CL1 scretion under homeostatic conditions (Kurth et al., 2001), The CCL20-CCR6 axis mediates dendritic cell localization, lymphocyte homeostasis, and immune responses in mucosal tissue (Cook et al., 2000). Regulatory T cells however, characterised by expression of CCR4, get positioned in lung and skin through secretion of CCL17 and CCL22 (Iellem et al., 2001, Sather et al., 2007).

Chemotaxis has also been shown to contribute significantly in malignant diseases. Tumor cells are able to attract immunosuppressive cells like Tregs or MDSCs leading to tumor growth and escape from immune control (Curiel et al., 2004, Schlecker et al., 2012, Chang et al., 2016, Chiu et al., 2016). The immunosuppressive tumormicroenvironment is thought to be one of the major issues regarding immunotherapy in form of adoptive cell therapy of solid tumors (Burga et al., 2015). However, there have been studies targeting and manipulating this effect. By artificial overexpression of CCR4 on cytotoxic $CD8^+$ T cells via transduction, it is possible to substantially improve adoptive cell therapy as more cytotoxic T cells are recruited into the tumor via CCL17 and CCL22 (Rapp et al., 2016). Similar studies have been performed with other individual chemokine receptors like CCR2 (Moon et al., 2011), CXCR2 (Peng et al., 2010) or CXCR6 (Lesch et al., 2021), thereby improving immunotherapy of malignant diseases. These studies showed that artificial overexpression of chemokine receptors on cytotoxic T cells can indeed improve immunotherapy against cancer. While multipe systematic expression and/or proteomic screens for chemokine *ligand* production in certain tumor models have been performed, to this date no holistic screening approach investigating chemokine *receptor* expression in T cells infiltrating a certain tumor model have been performed. Moreover, the effects of simultaneous artificial expression of more than one chemokine receptor on immunotherapy have never been investigated. To address these intriguing questions, a set of distinguishable marker proteins is required that allow for multiplexed transfer and in vivo

tracking of T cell populations transduced with distinct chemokine receptors or receptor combinations.

1.5 Multiplexed retroviral transductions as a tool to dissect immune cell migration, differentiation and proliferation

Ideally, an in vivo cell tracing technique comprises different important features. To allow for investigation of different leukocyte lineages, the expression of the used markers should not be lineage-specific but rather applicable to any immune cell. Furthermore, to address questions of lineage development over the course of numerous generations, stable inheritability is a key prerequisite. For single cell studies, clonal progeny can be retrieved in approximately 28% of initially transferred single cells (Buchholz et al., 2013). Therefore, in order to cumulate sufficient data in a justifiable amount of experimental animals, it is essential to have a high potential for multiplexing markers. Previous methods showed limitations regarding these terms. Cellular barcoding is based on DNA microarryay or next-generation sequencing and therefore includes cell lysis, consequently rendering further functional assays, like adoptive retransfers into secondary recipients impossible. Congenic markers on the other hand rely on a stable expression of the target protein and restrict usage from all non-expressing cell lineages. Furthermore, breeding and preservation of genetically compatible animals is a time and ressource consuming process. All above mentioned specifications could however be met by introducing the novel method of retrogenic color-barcoding (Grassmann et al., 2019) (Figure 1). This technique combines the method of generating bone-marrow chimeric mice (Holst et al., 2006) with transplantation of hematopoietic stem cells transduced with multiple fluorophore-encoding retroviruses. Transducing bone marrow with more than one fluorophore-encoding retrovirus at the same time results in a rich combinatorial barcode of distinctive cell tags, detectable on T cells, as well as B cells and NK cells (Figure 2). Combined encoding of color-barcodes and functional proteins, such as cell membrane receptors, adds another dimension to the technique. By transducing immune cells with markers co-expressed with functional proteins, it is possible to perform functional screenings in a multiplexed way (Figure 3). Consequently, retrogenic color-barcoding constitutes a novel tool in immunological research that allows studying fundamental cellular properties and lineage relations as well as performing multiplexed functional screens of candidate proteins – e.g. in the context of immunotherapy.

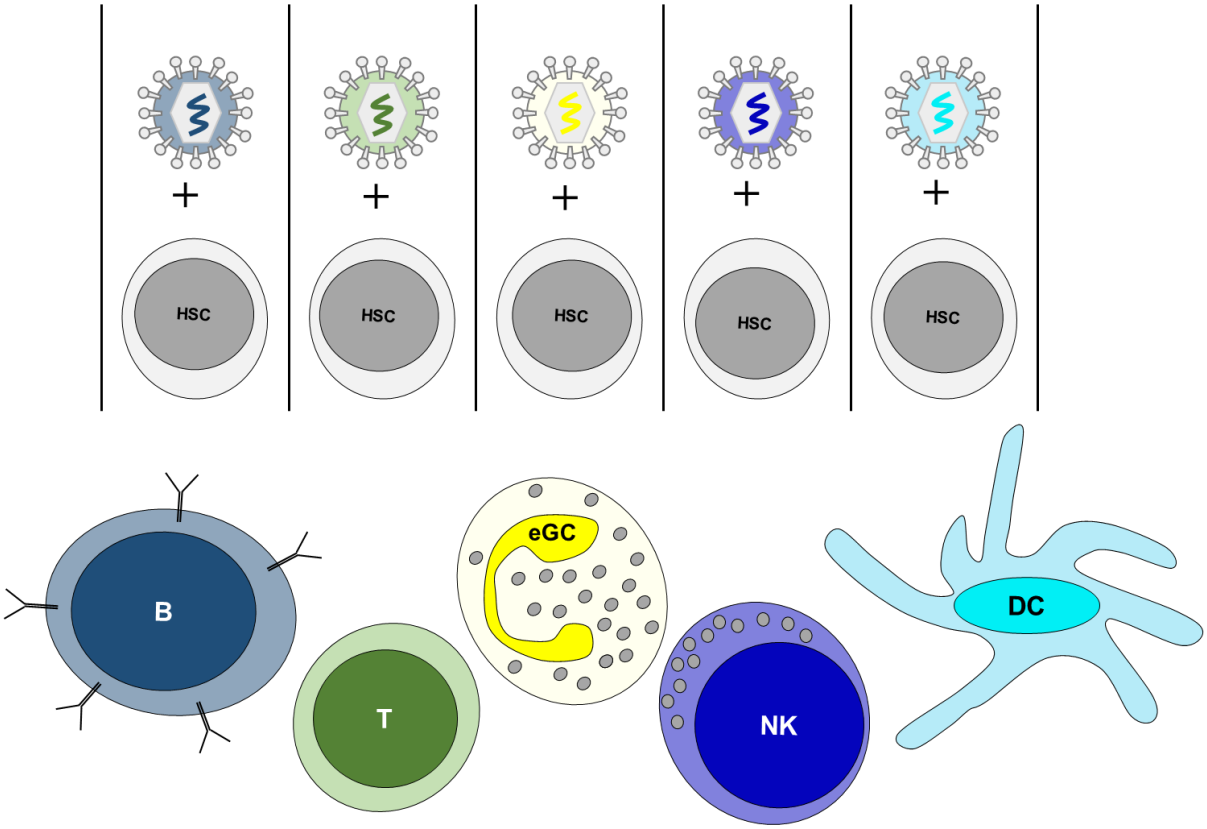

Figure 1 | Schematic representation of retrogenic color-barcoding.

Transduction of hematopoietic stem cells (HSCs) with fluorophore-encoding retroviruses leads to various color-barcoded immune cells. eGC = eosinophile granulocyte

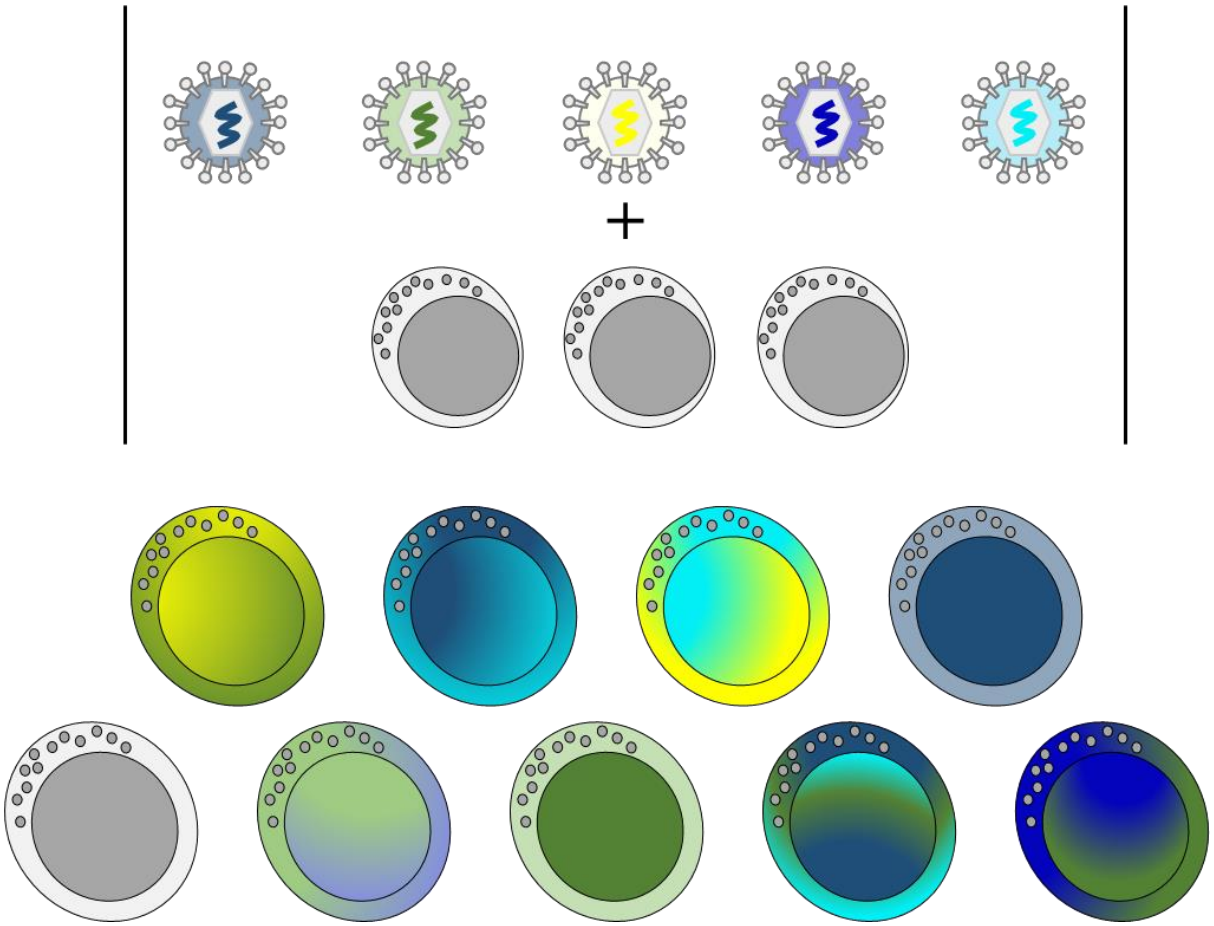

Figure 2 | Schematic representation of combinatorial transductions.

Simultaneous retroviral transduction of immune cells (e.g. NK cells) with different fluorophore-encoding retroviruses harbors various barcode possibilities due to combinatorial retroviral integration.

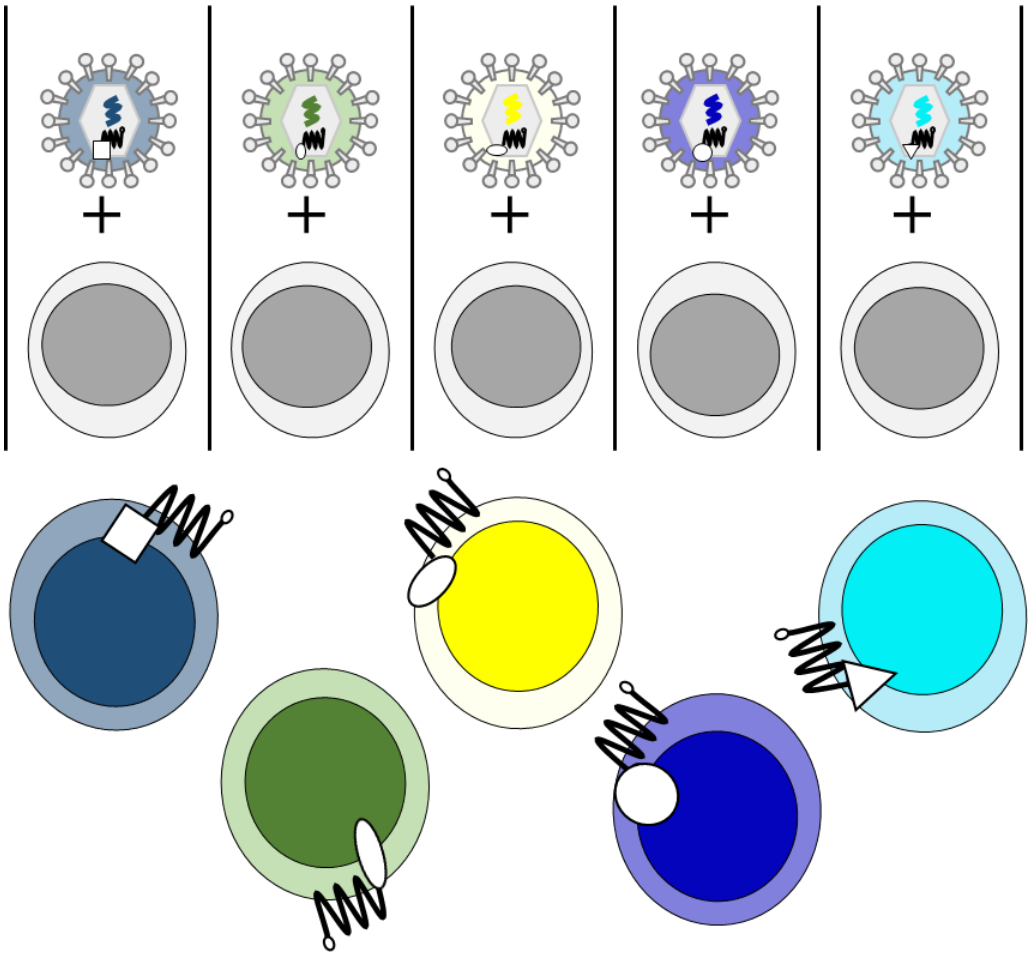

Figure 3 | Schematic representation of combined retroviral color-barcoding and functional modulation.

Transduction of immune cells (e.g. T cells) with retroviruses encoding for a fluorophore and a membrane protein (e.g. chemokine receptor) allows for tracking location and tissue accumulation of immune cells outfitted with a defined surface receptor.

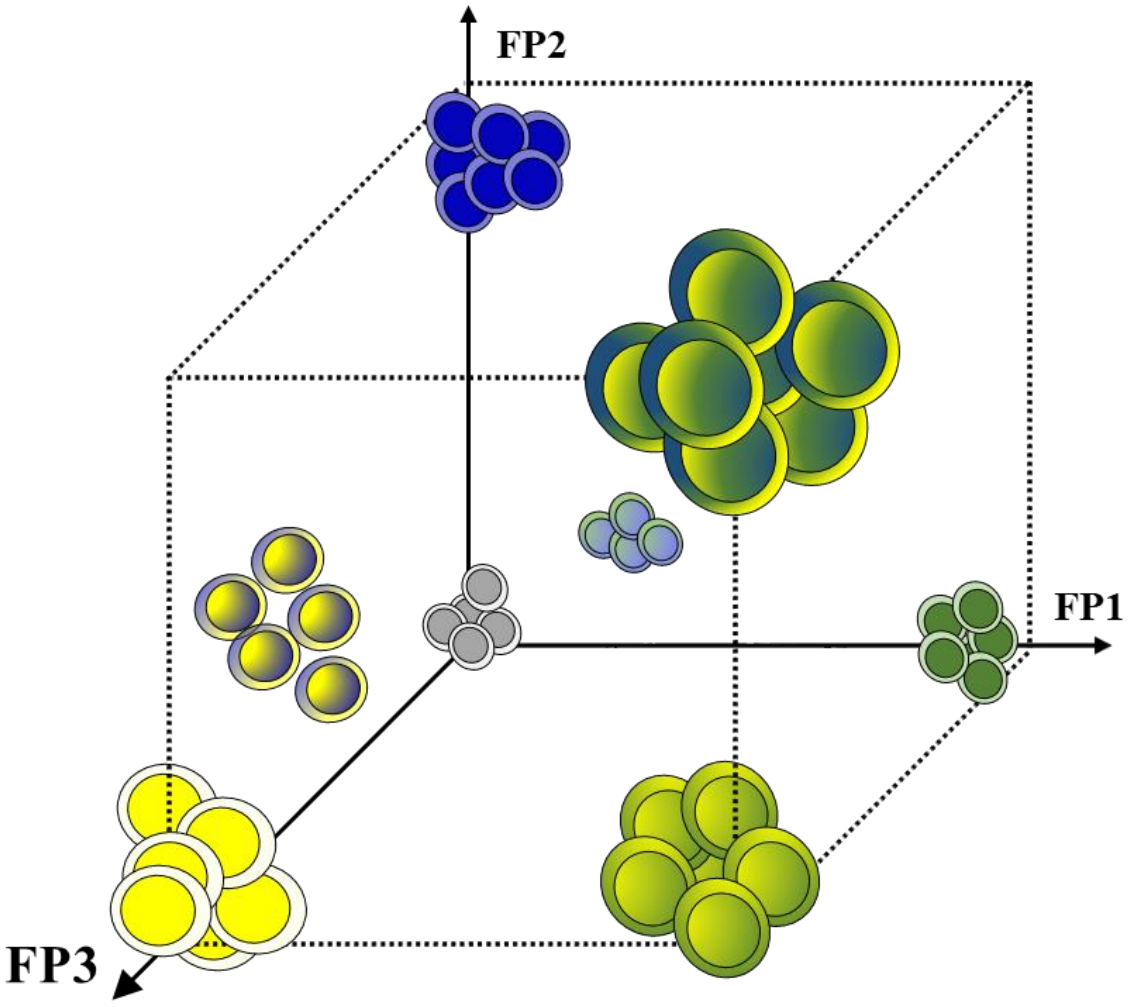

Figure 4 | Three-dimensional model of multispectral color-barcode analysis.

Each barcode can be discriminated based on its distinct spectral landmark. FP: fluorophore

2 Aim of this thesis

Fate mapping of immune cells and functional screens of immune cell function are key pillars of immunological research. However, multiplexing is key for both these methodical approaches in terms of efficient experiments. Moreover, comprehensive fate mapping and functional screening experiments require single-cell resolution as well as preservation of cell function. Most previous approaches, e.g. cellular barcoding or the congenic matrix, fail to meet these requirements. The introduction of retrogenic color-barcoding allows for a multiplexed analysis of live immune cell populations in fate mapping or functional screening experiments. In my publications, I demonstrate how the use of retrogenic color-barcoding can help us understand immunological mechanisms. The knowledge obtained by fate-mapping of even less investigated lineages like NK cells, as well as functional screening experiments can be used for the development of new drugs, vaccines and clinical studies.

The detailed aims of this thesis were to:

1) establish and verify the feasibility of retrogenic color-barcoding for in vivo experiments.
2) perform very first adoptive cell transfers of single NK cells in order to observe fundamental NK cell behavior, like proliferation, licensing and adaption to acute infection on a clonal level.
3) compare clonal properties of NK cells to T cell biology in a setting of acute viral infection, in terms of expansion capacity and adaptive shaping of their receptor repertoire.
4) implement retroviral color-barcoding in a study of chemokine receptor overexpression, in order to investigate migratory patterns of T cells in tumor diseases and assess the individual therapeutic effect of all murine chemokine receptors.
5) engineer T cells for adoptive therapy of tumor-bearing mice and identify optimal chemokine receptor profiles for improved therapeutic efficacy.

3 Methods

3.1 Mice

Mouse strain	Official name	Origin
C57BL/6	C57BL/6JOlaHsd	Envigo, Indianapolis, USA
OT-1	C57BL/6-Tg(TcraTcrb)1100Mjb/J	The Jackson Laboratory, Bar Harbor, USA
CD45.1	B6.SJL-Ptprca Pepcb/BoyJ	The Jackson Laboratory, Bar Harbor, USA
Rag2$^{-/-}$ Il2rg$^{-/-}$	C;129S4-Rag2tm1.1Flv Il2rgtm1.1Flv/J	The Jackson Laboratory, Bar Harbor, USA

6-12 weeks old female C57BL/6JOlaHsd were purchased from Envigo. 6-24 weeks old female SIINFEKL peptide-specific TCR transgenic OT-1 (C57BL/6-Tg(TcraTcrb)1100Mjb/J), 6-24 weeks old female CD45.1 (B6.SJL-Ptprca Pepcb/BoyJ) and 6-14 weeks old female and male Rag2$^{-/-}$Il2rg$^{-/-}$ (C;129S4-Rag2tm1.1Flv Il2rgtm1.1Flv/J) were originally obtained from The Jackson Laboratory and bred under specific pathogen-free conditions at our mouse facility at the Technical University of Munich. Approval for all animal experiments was granted by the district government of upper Bavaria (Department 5 – Environment, Health and Consumer Protection).

3.2 Tissue culture

58, Ba/F3-neo (WT), Ba/F3-m157, MC38-OVA, Panc02-OVA and Plat-E cells were grown in cDMEM in tissue culture – treated cell culture flasks. cDMEM was generated by supplementing DMEM with 10% FCS, 0.025% L-Glutamine, 0.1% HEPES, 0.001% gentamycin and 0.002% streptomycin. All cell lines, as well as transduced cells were incubated in humidified atmosphere at 37 °C and 5 % CO_2 and were split every 2-5 days depending on their confluence. Prior to splitting, MC38-OVA, Panc02-OVA and Plat-E were washed with PBS and afterwards treated with Trypsin-EDTA (5 min, 37 °C) to detach the cells from the bottom of the flask.

3.3 Generation of cell suspensions

3.3.1 Blood

Samples of 50 – 150 µl were collected in heparinized tubes by punction of the vena facialis using a 2.9 mm lancet. For optimal red blood cell lysis, the samples were resuspended in 15 mL tubes containing 10 mL ACT buffer, followed by an incubation of 10 min at RT and centrifugation for 7 min at 1500 rpm. After discarding the supernatant, lysis was repeated by resuspending the pellet in another 5 mL of ACT buffer and further 5 min of incubation at RT. Erythrocyte lysis was stopped by adding 5 mL cRMPI.

3.3.2 Spleen and lymph node

Spleens and lymph nodes were placed in a 60 mm petri dish containing 5 mL cRPMI and a 70 µm cell strainer. Homogenizing the whole organs resulted in a single cell suspension, which was transferred to a 15 mL tube. For collection of residual cells, both cell strainer and petri dish were rinsed with another 5 mL cRPMI. Centrifuging the transferred cells for 7 min at 1500 rpm resulted in a pellet, which was resuspended in 3 mL ACT buffer and incubated for 3 min at RT for red blood cell lysis. Adding 7 mL cRPMI stopped the lysis and cell numbers were determined in a Neubauer counting chamber, using Trypan Blue to identify and exclude dead cells.

3.3.3 Tumor infiltrating lymphocytes

Tumors were minced by scissors. Tumor tissue was digested with 1 – 1.5 mL RPMI 1640 supplemented with 1 mg/mL collagenase IV and 100 µg/mL DNAse I for 60 min at 37 °C. 10 mL of cRPMI were added to the digested tissue, followed by purification and transfer into a 15 mL tube through a 100 µm mesh. After centrifugation at 1500 rpm for 7 min, pellets were resuspended in 3 mL of 40 % Percoll solution and gradient centrifugation was performed at 2600 rpm and RT for 20 min (acceleration at 5/9 or medium, deceleration at 0/9 or minimal) to isolate lymphocytes. The lymphocyte fraction was washed with 10 mL PBS to remove remaining Percoll agent, followed by red blood cell lysis in 3 mL ACT buffer for 3 min at RT. Lysis was stopped by adding 7 mL cRPMI.

3.4 Inoculation of infectious and tumorous agents

3.4.1 Listeria

For bacterial infections, *Listeria monocytogenes* expressing Ovalbumin (*L.m.*-OVA, kindly provided by H. Shen, Philadelphia, USA) were used. Bacterial growth was initiated by incubation of 10 µl bacterial glycerol stock solution in 5 mL BHI medium at 37 °C while shaking at 90 rpm. OD measurements were done continuously to confirm exponential growth of the bacteria ($OD_{600} \approx 0.05$). Concentration was estimated from calibration curves using the formula $c=12x10^8xOD_{600}$ CFU/ml. Subsequently, bacteria were diluted in sterile PBS to reach the desired concentration of 10.000 CFU L.m.-OVA/mL. All steps after determining bacterial concentration were done at 4 °C to inhibit further bacterial growth. C57BL/6 mice were then intravenously administered 200 µl of diluted listeria to reach a primary infection dosage of 2.000 CFU L.m.-OVA.

3.4.2 MCMV

MCMV-WT and MCMV-IE2-SIINFEKL were kindly provided by Luka Cicin-Sain (Braunschweig, Germany). Upon adoptive transfer experiments, C57BL/6 and $Rag2^{-/-}$ $Il2rg^{-/-}$ were infected by intraperitoneal injection with 500.000 PFU MCMV-IE2-SIINFEKL and 50.000 PFU MCMV-WT (Smith strain), respectively.

3.4.3 Tumors

C57BL/6 recipients were irradiated at 4.5 Gy 24 hours prior to tumor implantation. MC38-OVA and Panc02-OVA were grown to 90% confluence and then brought into single cell suspension by washing with PBS and administering Trypsin-EDTA for 5 min at 37 °C. After detachment of adherent cells, cDMEM was added and cell numbers were determined in a Neubauer counting chamber, using Trypan Blue to identify and exclude dead cells. Tumor cells were resuspended in PBS to reach a concentration of $7.5x10^6$-$1x10^7$/mL. Recipient C57BL/6 were anesthetized in a chamber containing 1.5-5 % Isoflurane and subsequently injected s.c. at the right flank with 100 µl of tumor cell dilution to reach an inoculation dosage of $7.5x10^5$-$1x10^6$ cells per mouse. Tumor sizes, defined as tumor area (length x width), were measured every two to four days using a digital caliper.

3.5 Flow cytometry

Lymphocytes were isolated from respective organs as described and stained in a V-bottom 96 well plate. A maximum of $2x10^7$ cells were added per well and centrifuged at 1500 rpm and 4 °C for 3 min. Cell pellets were resuspended in 100 µl FACS buffer containing EMA (1:1000) for life/dead discrimination and anti-mouse CD16/CD32 antibody (1:500) for blocking of Fc receptors to avoid unspecific binding followed by incubation for 20 min at 4 °C exposed to light. Afterwards, cells were washed 1.5 times with FACS buffer and stained with respective antibodies diluted in 100 µl FACS buffer per well for 30 min at 4 °C in the dark. Cells were washed 2.5 times with FACS buffer and then either analyzed by flow cytometry or intracellular staining was performed. Transcription factor staining was done using eBioscience™ Foxp3 Transcription Factor Staining Buffer Set (Thermo Fisher) or True-Nuclear™ Transcription Factor Buffer Set (Biolegend) according to the manufacturer's instructions. Therefore, after final washing, cells were fixed in 200 µl Fixation/Permeabilization working solution for 30 minutes at 4 °C in the dark. Cells were centrifuged at 1800 rpm and 4 °C for 4 minutes and then washed with 200 µl 1X Perm Wash buffer. Intracellular staining was performed in 100 µl 1X Perm Wash buffer containing respective antibodies directed against transcription factors or Granzyme B at appropriate dilutions (30 min, 4 °C, in the dark). Finally, cells were washed 2.5 times with 1X Perm Wash buffer and resuspended in 200 µl FACS buffer for flow cytometric analysis.

3.6 Cell sorting and adoptive transfer of NK and T cells

3.6.1 Speed enrichment of NK cell sorting

To increase the percentage of $Ly49H^+$ NK cells from a splenic single cell suspension and thereby decreasing cell sorting time and preparation-related cell death, a stepwise FACS approach was chosen. Spleens of CD45.1 or retrogenic donor mice were prepared and brought into single cell suspension as described. After centrifugation for 7 min at 1500 rpm and 4 °C, the pelleted splenocytes were resuspended in 1 mL FACS buffer with anti-mouse NK1.1 antibody for 30 min at 4 °C protected from light. After washing with 10 mL cRPMI, cells were resuspended in 1 mL cRPMI. $NK1.1^+$ cells were enriched by flow cytometric sorting on a MoFlo XDP (Beckman Coulter, California, USA).

3.6.2 Cell sorting and adoptive transfer

Flow cytometric cell sorting was performed on a BD FACS Aria III (BD Biosciences, New Jersey, USA), MoFlo XDP or MoFlo Astrios cell sorter (Beckman Coulter, California, USA, both). For NK cells, speed enriched samples were washed with 10 mL FACS buffer and the cell pellet was resuspended in FACS buffer containing respective antibodies ($2x10^8$ cells/mL). For T cells, blood from OT-I donor mice was prepared as described. Surface staining was performed for 30 min at 4 °C protected from the light. Stained cells were then washed with 10 mL PBS and diluted in cRPMI without phenol red to a final cell density of $5x10^7$ cells/mL). PI was added 1:200 for life/dead discrimination. Cells were sorted in a V-bottom 96 well plate into 200 µl FCS containing either $2.5x10^5$-$5x10^5$ splenocytes from $Rag2^{-/-}$ $Il2rg^{-/-}$ for NK cell transfers or $2.5x10^5$-$5x10^5$ splenocytes from C57BL/6 for T cell transfers, serving as feeder cells respectively. Samples from retrogenic donors were further screened for individual color-barcodes based on their fluorophore expression pattern. Choosing distinct barcodes allowed for a multiplexed simultaneous sort of multiple barcoded single cells into the same well and thereby transfer into the same recipient mouse. Sorted NK cells were injected i.v. into the tail vein of $Rag2^{-/-}$ $Il2rg^{-/-}$ recipient mice. Sorted OT-I T cells were injected i.p. into C57BL/6 recipient mice.

3.6.3 Limiting dilution

Adoptive cell transfer of NK cells was performed in a multiplexed fashion by transferring multiple distinct barcoded cohorts into the same recipient. These cohorts consisted of 1, 5 or 10 single cells expressing the same distinct barcode in order to reduce the number of required recipient mice. Analyzing 1-cell derived progeny at d8 and d10 post infection revealed a likelihood to retrieve a single transferred cohort of 3.1 % and 1.24 %, respectively. Given these single cell recovery rates, the likelihood to recover progeny showing a defined barcode at d8 p.i. after tranfer of a 5-cell cohort should increase to approximately 15 % ($= 1–(1–0.031)^5$). Similiarly transferring a 10-cell cohort should increase the recovery rate of a defined barcode at d10 p.i. to approximately 12 % ($= 1–(1–0.0124)^{10}$). These predicted recovery rates were well in line with the actual recovery rates of a 5-cell or 10-cell cohort at d8 or d10 p.i., respectively. According to binomial distribution, 94% of 5- and 10-cell cohort-derived progenies can be expected to be truly single-cell derived. In this experimental setting, limiting dilution allowed for an at least fivefold reduction of required recipient mice.

3.7 Fluorescent barcoding

3.7.1 Isolation and color-barcoding of murine chemokine receptors

Single cell suspensions from C57BL/JOlaHSd tissue samples (spleen, lymph node, Peyer's plaque) were resuspended in 1 mL TRI Reagent, briefly incubated and 200 µL chloroform was added. Phase separation was performed at 12000 g for 15 min at 4 °C in a tabletop centrifuge. RNA precipitation was achieved by addition of 500 µL isopropanol to the upper layer after phase separation. The RNA pellet was washed with 1 mL 4 °C 70 % ethanol. Primers for each of the 18 known signaling murine CRs were designed by referring to the NCBI's database and generated by Eurofins Genomics. Reverse transcription was performed with 5 µg of the isolated total RNA using the AffinityScript cDNA Synthesis Kit. All fusion constructs of murine CRs and FPs were generated by overlap extension PCR and cloned into the retroviral pMP71 vector (a kind gift from Wolfgang Uckert) for recombinant expression in target cells.

3.7.2 Transfection of virus-producing cell lines

Transfection of retroviral vectors encoding for either the five fluorescent proteins GFP, YFP, T-Sapphire, CFP and BFP (color barcoding) or the barcoded chemokine receptors was achieved by calcium phosphate precipitation. Therefore, Plat-E were seeded in 6 well plates and grown for 2-3 days until reaching 70 % confluence. 18 µg of the retroviral plasmid was dissolved in 135 µl ddH_2O and mixed with 10 % of a 3.3 M $CaCl_2$ solution. The mixture was added dropwise to an equal volume of transfection buffer while vortex mixing. After incubation for 30 min at RT including vortex mixing after 15 min, the precipitate was carefully distributed onto the seeded cells using a P1000 pipet. After 6 h, medium was removed from the cells and fresh cDMEM was added. Viral supernatant was collected after 48 and 72 h, purified from remaining cells by centrifugation for 7 min at 1500 rpm and 4 °C. Transfection efficacy was measured via flow cytometry after 2 days. The harvested virus supernatants were stored at 4 °C and used within 4 weeks.

3.7.3 Retroviral transduction of T cells

Stable integration of retroviral DNA plasmids was achieved by spinoculation. Retroviral supernatant was either used directly or mixed for multiple (combinatorial transduction) constructs per well. For transduction of 58 cells, 400 µl of viral supernatant was added to each

well of a tissue-culture treated 48 well plate and centrifuged for 2 h at 3.000 g and 32 °C. Then, 25.000 cells were added in 50 µl cDMEM to each well and the plate was spun again for 90 min at 800 g and 32 °C. For transduction of murine splenocytes, a single cell suspension of spleens from OT-I donors was prepared as described, splenocytes were distributed in a tissue-culture treated 6 well plate at a concentration of 2.000.000 cells/mL cRPMI and stimulated with IL-2 (25 U/ml), anti-CD3 (1:1000) and anti-CD28 (1:5000) antibodies for 18-24 hours. A tissue-culture untreated 24-well plate was coated overnight at 4 °C with 250 µl PBS per well, containing RetroNectin (1:100), anti-CD3 (1:1000) and anti-CD28 (1:5000) antibodies. At the day of transduction, coating of the plate was removed by washing once with PBS and 1 mL of viral supernatant (color barcodes or barcoded CRs) was added before centrifugation for 2 h at 3.000 g and 32 °C. After removing the viral supernatant, stimulated splenocytes were added ($5x10^5$ cells/mL cRPMI with 25 U/mL IL-2), spun again for 90 min at 800 g and 32 °C. Following transduction, all cells were taken into tissue culture.

3.7.4 Generation of retrogenic mice

8-20 weeks old donor mice were sacrificed (CD45.1 or C57BL/6 mice for NK cell, CD45.1 Rag-$1^{-/-}$ OT-1 for T cell retrogenic mice). Femora and tibiae of the donor mice were removed and prepared. Bone marrow cells were harvested by opening the bones at both diaphyses and flushing the bone marrow cavity with 3 mL cDMEM per bone by using a 5 mL syringe and a 26G needle. Cells were centrifuged at 1500 rpm for 7 min and resuspended in 3 mL ACT buffer for 3 min at RT. Red blood cell lysis was stopped by adding 7 mL cDMEM. Afterwards, bone marrow cells were brought into single-cell suspension and stained with anti-mouse CD3/19 and anti-mouse Ly6A/E (Sca-1) antibodies in 500 µl FACS buffer for 30 min at 4 °C protected from light. After incubation, cells were washed with 10 mL FACS buffer and resuspended in 500 µl cDMEM for FACS. PI was added (1:200) for life/dead discrimination. Sca-1^+ $CD3^-$ $CD19^-$ HSCs were sorted into FCS and afterwards washed with 5 mL PBS. Sorted cells were taken into tissue culture in cDMEM, supplemented with 20 ng/mL mIL-3, 50 ng/mL mIL-6 and 50 ng/mL mSCF (1x stimulation medium) and cultivated for 3-4 days in a tissue-culture treated 48 well plate ($2.5x10^5$-$3.5x10^5$ cells/400 µl). For retroviral transduction of the stimulated HSCs, a non-tissue culture treated 48 well plate was coated with RetroNectin in PBS (1:100) overnight at 4 °C. Viral supernatants were collected from Plat-E cells transfected with retroviral vectors encoding for the different FPs and pooled at individual concentrations depending on their transfection efficacy to achieve combinatorial transduction of the HSCs. Coating of the wells was removed by washing with PBS once. 400 µl of the pooled supernatants were added per

well and centrifuged for 2 h at 3.000 g and 32 °C. Stem cells were collected and resuspended in fresh 2x stimulation medium at a final concentration of $1.5x10^6$ cells/mL. After spinoculation, 200 µl of the viral supernatants were discarded and 200 µl of the prepared HSCs were added per well. After another spinoculation for 90 min at 800 g and 32 °C, the cells were taken into tissue culture for 2-3 days. After cultivation of the barcoded HSCs, C57BL/6 recipient mice were irradiated two times at 4.5 Gy with 4 h in between using a cesium irradiator. Mice were therefore put into beakers laid out with litter and closed with breathable filter paper. After the second irradiation, cells were collected, washed with 10 mL PBS and resuspended in FCS at a final density of $5x10^6$-$1x10^7$ cells/mL. 100 µl of the cell suspension were injected i.v. into the irradiated recipients. Chimerism of the retrogenic mice could be determined after 4 weeks in peripheral blood samples via flow cytometry.

3.8 Functional assays

3.8.1 Ba/F3 co-culture

Ba/F3-neo (WT) and Ba/F3-m157 were a kind gift from Hisashi Arase and Lewis Lanier. Both cell lines were transferred to 15 mL tubes and cell numbers were determined using a Neubauer counting chamber. Ba/F3 cells were centrifuged at 1500 rpm for 6 min and resuspended in cRPMI with a final cell density of 2.5 x 10^5 cells/mL. 50.000 cells were added per well to a u-bottom 96 well plate in cRPMI and co-incubated for 12 hours with 5.000 or 10.000 Ly49H^{hi} or Ly49H^{lo} NK cells sorted from spleens of CD45.1 mice. For resting, cells were stained with anti-CD45.1 antibodies and sorted into new wells containing 400.000 Ly49H$^{-/-}$ splenocytes in cRPMI containing 25ng/mL mIL-15 (PeproTech) and 25U/mL hIL-2 (PeproTech). After two days of culture, cells were harvested, stained with respective antibodies and analyzed via flow cytometry.

3.9 Statistics

Prism software (v9.1.0, GraphPad) was used for quantification and statistical analysis. Normality tests were performed to decide whether to use parametric or nonparametric tests, where applicable. Significances were calculated using unpaired *t*-test and Mann-Whitney test,

survival differences were approached using Log-rank test. Correlations were measured as Spearman correlations. Significance is defined as *p-value < 0.05, **p-value < 0.01, ***p-value < 0.001, ****p-value < 0.0001. Cluster analysis was performed by fitting Gaussian mixture models to logarithmically transformed parameters, further optimized by using the Expectation-Maximization algorithm as implemented in the function ‘fitgmdist’ of MATLAB’s ‘Statistics and Machine Learning Toolbox’. Covariance matrices were assumed full but identical for all components before determining the number of clusters based on the Bayesian Information Criterion. Experimental parameters were then assigned to the component with the highest posterior probability.

4 Summary of the presented publications

4.1 Distinct Surface Expression of Activating Receptor Ly49H Drives Differential Expansion of NK Cell Clones upon Murine Cytomegalovirus Infection

In this publication (Grassmann et al., 2019) we investigated if individual NK cells share certain features with the adaptive immune system, although being canonically allocated to the innate immune system. Previous work had shown intriguing parallels of NK cells, harboring the activating NK cell receptor Ly49H that recognizes an MCMV-encoded glycoprotein, to $CD8^+$ T cells. Like $CD8^+$ T cells, these $Ly49H^+$ NK cells show population expansion, contraction and long term persistence after initial antigen encounter during MCMV infection (Sun et al., 2009). Furthermore, $CD8^+$ T cells have been shown to adaptively shape and focus their epitope-specific TCR repertoire upon rechallenge with the same pathogen, resulting in an epitope-specific affinity maturation (Busch et al., 1998, Busch and Pamer, 1999). Interestingly, similar processes have been suggested to occur in $Ly49H^+$ NK cells, e.g. by selection and expansion of cells with defined receptor combinations (Orr et al., 2010, Nabekura and Lanier, 2016). If such processes were to occur, focusing to certain NK cell clones that heritably express certain receptor combinations should be observed. In order to study such clonal NK cell dynamics, we introduced the method of retrogenic color-barcoding as a novel approach for in vivo fate mapping of individual NK cells and their progeny.

Being able to detect single-cell derived $Ly49H^+$ NK cell progeny upon infection with MCMV, we could show that NK cell responses vary substantially in size, comparable to variation in immune response sizes derived from individual $CD8^+$ T cells (Buchholz et al., 2013). Interestingly, increasing size of clonal responses correlated with a more differentiated phenotype, suggesting a coupling of clonal expansion and NK cell maturation over the course of infection.

Next, we asked whether the additional expression of inhibitory receptors of the Ly49 family (namely Ly49A, Ly49C/I, and Ly49G2) would influence NK cell response size. Throughout clonal expansion, stable expression of each above mentioned receptor was maintained. Interestingly, only licensing-relevant Ly49C/I showed clonal restriction of expression upon acute infection, whereas gain of expression could be observed for Ly49A and Ly49G2. Surprisingly, neither of the above mentioned phenotypes influenced the response size of individual NK cells.

Thereafter, we hypothesized wether the density of Ly49H expression might influence the degree of clonal expansion. Strikingly, we found distinct levels of said expression that were in line with clonal response size. Following individual NK cells of high or low Ly49H density over the course of infection unveiled that – despite transient downregulation – such distinct expression levels are indeed clonally maintained throughout expansion and contraction phases. This was in line with work of colleagues, showing a functional distinction and avidity selection of different expression levels of Ly49H (Adams et al., 2019). These findings argue that NK cells do have the capacity to adapt to infectious agents by selecting for NK cells with high expression of Ly49H, mirroring the repertoire focusing and affinity maturation of T cell clones over the course of infection.

For this publication, I co-developed and optimized retrogenic color barcoding for in vivo fate mapping of NK cells upon MCMV infection. I performed and analyzed key in vitro and in vivo experiments and co-wrote the manuscript.

4.2 Unbiased chemokine receptor screening reveals similar efficacy of lymph node- and tumor-targeted T cell immunotherapy

In this publication (Pachmayr et al., 2023) we investigated the therapeutic potential of engineering T cells with chemokine receptors to overcome insufficient migration of T cells during adoptive cell therapy of solid tumors. While adoptive cell therapy has had a great therapeutic impact in the treatment of haematologic malignancies (Neelapu et al., 2017, Maude et al., 2018), treating solid tumors with this method has proven much more difficult. Most likely, this is because solid tumors create an immunosuppressive microenvironment by releasing chemokines that fail to attract anti-tumoral cytotoxic immune cells and instead recruit protumorigenic cells into the tumoral stroma (Curiel et al., 2004, Schlecker et al., 2012, Chang et al., 2016). Accordingly, previous work showed significant therapeutic success of artificial overexpression of certain chemokine receptors in tumor-specific T cells (Peng et al., 2010, Moon et al., 2011, Rapp et al., 2016, Lesch et al., 2021). However, these studies evaluated delibaretly chosen single receptor candidates, thus examining merely a fraction of the known chemokine receptor family, as well as sparing possible receptor combinations. To overcome these limitations, we created a transducible retroviral library of all known murine chemokine receptors and coupled it to our color-barcode. This enabled us to directly test the ability of T cells, transduced with individual chemokine receptors or receptor combinations, to invade subcutaneously injected carcinoma models and test for their therapeutic impact.

Utilizing the aformentioned method of retroviral color-barcoding, each transduced chemokine receptor was tagged with a specific fluorophore. Retroviral combinatorial transduction in combination with congenic markers, in an adoptive transfer system using tumor-specific OT-I T cells, allowed for the investigation of up to 8 individual chemokine receptors per recipient mouse. Analyzing different organs in OVA-antigen expressing tumor-bearing mice at an early timepoint after T cell infusion defined characteristic organ homing patterns conveyed by each chemokine receptor.

Furthermore, evaluation of tumors and tumor-draining lymph nodes showed receptors that drive differential homing into each of these organs. We assembled the chemokine receptors with the highest infiltration into these pivotal therapeutic target organs and assigned these to a tumor-homing (CCR6, CXCR1, CX_3CR1) or a lymph-node homing (CCR4, CCR7) batch. Both T cells engineered with the tumor or the lymph node homing batch showed enhanced therapeutic efficacy compared to untreated mice as well as mice receiving an infusion of fluorophore-

transduced OT-I cells without chemokine engineering. Analyzing the migration and phenotype of transferred T cells over the course of time showed a prefential enrichment of the tumor batch-tranduced cells into the tumor, while the lymph node batch-transduced ones displayed better persistance and higher expression of markers for T cell stemness.

Next, we hypothesized that simultaneous expression of chemokine receptors with elevated capacity for tumor or draining lymph node infiltration would lead to even better organ-specific migration and an improved therapeutic effect of transferred cells. Therefore, we compared OT-I T cells transduced with one or multiple distinct chemokine receptors per cell at different time points after treatment. Surprisingly, no clear synergistic migratory effect could be observed evaluating both tumor- and lymph node-directed transduction. Investigating their individual therapeutic potential, CCR4-transduction showed a clear benefit in terms of survival in line with previous findings (Rapp et al., 2016), whereas CCR7-transduction showed no therapeutic effect at all. Further investigating this intriguing difference, we compared PD-1 expression of both groups. While CCR4-transduced cells showed an elevated expression in comparison to non-chemokine receptor engineered transferred T cells, CCR7-transduced cells showed even lower expression of PD-1 than these control cells. As PD-1 is induced by antigen receptor signaling (Lu et al., 2014) and serves as early activation marker, these findings suggested that CCR7 overexpression potentially impaired antigen recognition whereas CCR4 facilitated stromal intercellular interaction within the tumor microenvironment, which is in line with previous work (Rapp et al., 2016). Consequently, lymph node targeting per se seems not to be the key. Instead, thereapeutic efficiency may depend on the specific cellular interactions a certain chemokine receptor enables within the lymph node.

Lastly, we decided to test a simultaneous implementation of both tumor and lymph node targeting, driven mainly by CCR4 and CCR6. While both individual strategies showed a clear therapeutic effect, simultaneous expression of CCR4 and CCR6 in transferred T cells lead to loss of this survival benefit. As PD-1 analysis of CCR6 in tumors showed a comparably elevated expression as for CCR4 in lymph nodes, we hypothesized that combining both strategies would lead to enhanced exhaustion caused by additive PD-1 upregulation. Indeed, phenotypic analysis of CCR4/CCR6 double-transduced cells showed significantly elevated levels of PD-1 compared to CCR6-driven lymph node infiltration, implicating an exhausted phenotype.

Taken together, these findings indicate that adoptive cell transfer of solid tumors can be improved by chemokine receptor engineering. Furthermore, direct targeting of the tumor as well as tumor-draining lymph nodes proved to be promising approaches. However, future work

requires a more detailed assessment, whether expression of more than one chemokine receptor or combination with established immunotherapies such as checkpoint blockade can further increase therapeutic efficacy.

For this publication, I co-developed and optimized retrogenic color barcoding for in vivo mapping of migration patterns in anti-tumoral T cells. I performed and analyzed key in vitro and in vivo experiments and co-wrote the manuscript.

5 Discussion

5.1 Multiplex analysis for in vivo fate mapping & functional screens

Multiplex analysis using retrogenic color-barcoding has proven to be a novel and variable asset to tackle immunological questions. On the one hand, it enables thorough investigation of individual immune cell fates. Ly49H$^+$ NK cell clones showed an intriguing variation in their response size to acute infection with MCMV. Such diverse clonal output has previously been observed for other adaptive immune cells, like CD8$^+$ T cells (Buchholz et al., 2013). Innate immune cells like NK cells however were expected to respond more uniformly. Furthermore, clonal modulation of the NK cell response against MCMV proved to be influenced by the expression level of Ly49H. This implicates directed selection and adaption within the NK cell compartment during acute infection based on antigen-specific receptor expression, thereby optimizing overall functional avidity. These findings again show striking parallels to the repertoire focusing and affinity maturation of specific T cell clones (Busch and Pamer, 1999). Taken together, these results put NK cells in a new perspective within the cellular immune response, bridging adaptive and innate immunity. Further studies will help elucidate NK cell characteristics in comparison to T cell biology, as well as other less investigated cell lineages, harboring novel therapeutic applications in the context of drug development and adoptive cell therapy.

On the other hand, multiplex analysis can not only be used for fate mapping, but also to evaluate functional capacities and therapeutic modifications of various cell types. By coupling the fluorophores to specific proteins like transmembrane receptors, the target cells are not only functionally modified, but also color-barcoded at the same time. Multiplexing based on our technique enabled us to transfer differently modified cells simultaneously into the same recipient to reduce experimental animal numbers. Even a modulation of target cells with multiple different proteins at the same time could be achieved, thus allowing for the study of the functional impact of both individual targets and target combinations. Previous work in the context of adoptive cell therapy focused on individual targets like single chemokine receptors (Peng et al., 2010, Moon et al., 2011, Rapp et al., 2016, Chow et al., 2019, Di Pilato et al., 2021). Due to our novel approach, for the first time we were able to comprehensively survey the migratory effect and therapeutic potential of the entire chemokine receptor family against a specific tumor entity. In this manner, future studies may address a variety of tumor entities apart

from murine carcinoma. Having established a library of all human chemokine receptors, future work will enable us to adopt our approach to assess also human cancer entities in humanized mice. Doing so will allow us to put our findings in a more translational perspective and propose modulations of established clinical cell products.

Moreover, retrogenic color-barcoding adds the possibility to not only assess clonal fates and functional modulations, but also phenotypic features of target cells. When we design a library of combinable fluorophores, a reasonable balance between the variety of potential color barcodes and spectral latitude for phenotypic analyses is required. Studying the target cells with a multiple-laser flow cytometer requires thorough optimization of the applied spectral filters and fluorophores. Our experimental setup allowed us to leave two laser wavelengths open for phenotypic flow cytometric analysis, while employing two other lasers for the detection of the multiplexed color barcodes. As modern flow cytometers are steadily being optimized and equipped with more lasers and individual filter settings, the potential to further enlarge data output grows concurrently. The same holds true for novel fluorescence spectrum analyzers. Pushing the limits of the optical spectrum, including even ultraviolet and infrared wave lengths, adds a new level of flexibility. This will allow us to either add more fluorophores to the library to increase the number of potential barcodes or perform more in-depth phenotypic analyses in the future.

Thus, due to its high analytical output as well as the potential for phenotypic analysis of live cells, application of retrogenic color-barcoding has a great potential for the study of other open immunological questions in immunology research.

5.2 Alternative applications of retrogenic color-barcoding

Tracing individual clones, we were able to elucidate fundamental mechanisms of NK cell biology. Moreover recently, we could use single cell fate mapping via retrogenic color-barcoding to characterize a novel ILC1-like NK cell subset, bridging innate and adaptive immunity (Flommersfeld et al., 2021). These NK cells show characteristics reminiscent of ILC1, such as broad cytokine production and tissue residence, as well as features canonically attributed to NK cells such as target-specific cytotoxicity, interaction with dendritic cells and adaptive-like response patterns to infection.

Recent studies also shed light on additional features of NK cells that resemble other immune cell lineages, such as longevity, antigen specificity and formation of immunological memory. Following this thought, future work might enable the field to clonally investigate and assess formation of NK cell memory, a phenomenon that has first been observed for T cell- and B cell-independent NK cell responses to haptens (O'Leary et al., 2006) and later found in CMV infection both in mice and humans (Sun et al., 2009, Hammer et al., 2018, Rückert et al., 2022). To date, studies concerning NK cell memory are primarily performed with NK cell populations. However, true immunological memory requires that specific criteria are met (Murphy et al., 2022). First, a single cell and its progeny must be able to expand and react upon primary antigen exposure, before contracting again and persisting after antigen clearance. Then upon secondary challenge with the same antigen, single long-lasting progeny cells of the original clone must mount the secondary expansion. Retransferring single cell descendants into a secondary recipient followed by immunization after the initial clonal response in a primary host might be a way to test for true NK cell memory.

Another benefit of retrogenic color-barcoding is its applicability for different immunological lineages and infection settings. Besides individual NK cell responses to acute virus infection, our method was also adapted to study clonal T cell responses in chronic virus infection (Grassmann et al., 2020). It helped not only to generate a large quantity of traceable T cell clones. Furthermore, the fluorescent labels proved to be distinct and traceable even after more than 200 days, as well as after retransfer and rechallenge in a secondary recipient. In this study, mapping individual T cell clones showed that long-term persistence of its progeny during chronic infection is determined during the acute phase of infection, however it is not predicted by the degree of acute clonal expansion. Instead, the higher the abundance of central memory precursor cells in T cell families during acute infection, the bigger the magnitude of memory inflation during chronic infection. Such long-term studies allow for further insights in formation and capacity of immunological memory regarding different immune cells.

Moreover, retrogenic color-barcoding holds the potential to combine fate mapping with functional screens. Recent studies focused on T cell exhaustion of individual clones in chronic LCMV infection. Utilizing our technique, the transcription factor Myb showed to play a key regulator role orchestrating T cell exhaustion and the response to checkpoint inhibition (Tsui et al., 2022). In similar work, transcriptomics showed a reciprocal relationship between both transcription factors Stat5a and Tox, monitoring the phenotype of exhausted $CD8^+$ T cells between progenitor and terminal subsets in chronic viral infection and cancer (Beltra et al.,

2022). Targeted Stat5a signaling restrains Tox activity, supports an effector instead of exhaustion epigenetic landscape, drives a durable and protective T cell differentiation and is essential for T cell response to therapeutic PD-L1 blockade. To date, our studies of functional T cell modulation focused on membrane-bound receptors. Future functional screens can be used to study other types of proteins, such as transcription factors. Examining multiple transcription factors via multiplexing might lead to new promising candidates to optimize the T cell response in pathological conditions. Beyond that, equipping T cells with intra- and extracellular features simultaneously and thus combining both approaches is possible. Hence, future work will have essential impact on the development of new therapeutic strategies that can optimally harness the potential of the immune system against chronic infection and cancer.

5.3 Limitations of retrogenic color-barcoding

Retrogenic color-barcoding has limitations that should be overcome in the future. Generation of retrogenic mice is a time and resource consuming process. Sufficient tissue engraftment in retrogenic donor mice is usually observed after up to 4-5 weeks. Poor transduction efficacy and impaired bone marrow engraftment are issues that can lead to insufficient retrogenic engraftment and need to be further optimized. Moreover, harvesting immune cells outside the blood circulation at sufficient numbers (like e.g. NK cells, Tregs or DCs) requires major interventions like a partial splenectomy or surgical lymph node removal, if not euthanasia.

Another issue is the potential immunogenicity and cellular toxicity of fluorophores (Ansari et al., 2016). Preclinical studies testing proteins of the GFP family for gene therapy and clinical trials showed that peptide presentation of GFP derivatives via MHC can lead to T cell-mediated immunogenicity in certain mouse strains, especially BALB/c (Stripecke et al., 1999, Gambotto et al., 2000). This limits the application of color-barcoding to other strains like C57BL/6 (Skelton et al., 2001). Breeding of GFP-tolerant strains (e.g. GFP-reporter strains) represents one possible solution, as well as immunodeficient mice.

Finally, retroviral vectors are randomly integrated into the host's genome, which can lead to insertional mutagenesis with severe outcomes (Li et al., 2002, Hacein-Bey-Abina et al., 2003). Alternatively, lentiviral vectors can transduce even quiescent cells and are integrated in a more controlled fashion into the host cell's genome (Mitchell et al., 2004). However, there are still reports of insertional mutagenesis using lentiviral vectors in experimental and clinical studies (Cavazzana-Calvo et al., 2010, Ranzani et al., 2013). This can lead to uncontrolled target cell

proliferation and leukemia in retrogenic mice. Furthermore, random integration of retroviral vectors can impair the functional capacities of the host cell. Especially in multiple transductions required for multiplexing, insertional mutagenesis and functional disruption become even more likely. A possible way to circumvent these unpredictable events is gene editing via CRISPR-Cas9, allowing for a targeted genomic integration (Doudna and Charpentier, 2014). This method has been shown to effectively edit the host cell's genome, leading to groundbreaking developments in the field of gene therapy while having a better safety profile (Rupp et al., 2017, Newby et al., 2021).

In summary, retrogenic color-barcoding as a preclinical labeling tool shows a great potential for further single-cell investigations, as well as functional screens. However, the use of this method in a more efficient way requires further optimization. Moreover, technological refinement to alleviate safety concerns will be required for possible applications in translational and clinical studies.

5.4 Single-cell sequencing as a future direction of fate mapping

Recently, single cell RNA sequencing (scRNAseq) revolutionized the field of lineage development and tracing. Breaking down genetic information of individual cells revealed numerous novel immune cell subsets and their relationships to each other and non-immune cells. This method and its refinement over the past decade changed a time-consuming and expensive application into affordable high-throughput technologies, enabling researchers to assess thousands of individual cells simultaneously (Fan et al., 2015, Cao et al., 2017, Jovic et al., 2022). Nowadays, whole tissues and organs rather than cell populations can be studied at single-cell resolution.

At the same time, scRNAseq integrates the potential for clonal analyses. As each naïve T cell harbors its own unique TCR sequence (Davis and Bjorkman, 1988), it can serve as a distinct label for itself and its progeny (Stubbington et al., 2016). Cell types without such a genetic label can be tagged alternatively as well. Referring to retrogenic color-barcoding and subsequent flow cytometric analysis, mRNA barcoding represents a high-throughput and accurate approach that similarly enables individual genetic cell analysis via scRNAseq (Klein et al., 2015, Macosko et al., 2015). Recently, CRISPR-Cas9 gene editing presented another sophisticated method to induce 'genetic scars' in individual cells, caused by short genetic insertions and deletions in non-functional genomic sections (Spanjaard et al., 2018). First realized in zebrafish,

the development of a new mouse line now also enables murine lineage studies based on DNA scarring (Bowling et al., 2020). Equipping target cells with such individual genetic barcodes allows for distinction of thousands of cells when analyzing transcriptomic single cell data (Guo et al., 2019).

Along the way, generating a vast amount of data placed particular emphasis on data analysis and computational biology. Machine learning revolutionized the field of genomic data analysis and interpretation (Eraslan et al., 2019). Deep neural networks as the state-of-the-art technology exploits the advantages of algorithmic advances and increasing computational capacity, enabling the field to comprehensively and quickly analyze highly complex data within a reasonable time period. However, tissue preparation for transcriptomics like scRNAseq includes deterioration of three dimensional and spatial information (Papalexi and Satija, 2018). In response, further development introduced the method of spatial transcriptomics. This technique repeats targeted scRNAseq on multiple morphological tissue layers in order to provide spatial blueprints, virtually reconstructing the genetic architecture of target tissues (Vickovic et al., 2019). Growing comprehension of data handling even led to the addition of RNA velocity to single cell analysis (Bergen et al., 2020). This set of information is based on the rate of gene expression at a given time point, referring to the ratio of its spliced and unspliced mRNA. Comparing between multiple single cells, dynamic gene expression can be assessed and visualized. This part of data analysis gathers further essential cellular and intercellular information and thereby adds another temporal dimension to an already powerful tool.

In summary, novel methods using single-cell transcriptomics have the potential to overcome some limitations of previous methods. Their development, integration and improvement contribute profoundly to better understand physiological relations, pathological processes and how to cure various diseases. However, since RNA or DNA have to be isolated for these methods, assays that require live cells cannot be replaced with such methods.

6 Bibliography

Adams, N. M., Geary, C. D., Santosa, E. K., Lumaquin, D., Le Luduec, J. B., Sottile, R., Van Der Ploeg, K., Hsu, J., Whitlock, B. M., Jackson, B. T., Weizman, O. E., Huse, M., Hsu, K. C. & Sun, J. C. 2019. Cytomegalovirus Infection Drives Avidity Selection of Natural Killer Cells. *Immunity,* 50**,** 1381-1390 e5.

Ansari, A. M., Ahmed, A. K., Matsangos, A. E., Lay, F., Born, L. J., Marti, G., Harmon, J. W. & Sun, Z. 2016. Cellular GFP Toxicity and Immunogenicity: Potential Confounders in in Vivo Cell Tracking Experiments. *Stem Cell Rev Rep,* 12**,** 553-559.

Ara, T., Tokoyoda, K., Sugiyama, T., Egawa, T., Kawabata, K. & Nagasawa, T. 2003. Long-term hematopoietic stem cells require stromal cell-derived factor-1 for colonizing bone marrow during ontogeny. *Immunity,* 19**,** 257-67.

Araki, K., Turner, A. P., Shaffer, V. O., Gangappa, S., Keller, S. A., Bachmann, M. F., Larsen, C. P. & Ahmed, R. 2009. mTOR regulates memory CD8 T-cell differentiation. *Nature,* 460**,** 108-12.

Battaglia, M., Stabilini, A. & Roncarolo, M. G. 2005. Rapamycin selectively expands CD4+CD25+FoxP3+ regulatory T cells. *Blood,* 105**,** 4743-8.

Becker, A. J., Mc, C. E. & Till, J. E. 1963. Cytological demonstration of the clonal nature of spleen colonies derived from transplanted mouse marrow cells. *Nature,* 197**,** 452-4.

Bergen, V., Lange, M., Peidli, S., Wolf, F. A. & Theis, F. J. 2020. Generalizing RNA velocity to transient cell states through dynamical modeling. *Nature Biotechnology,* 38**,** 1408-1414.

Biron, C. A., Byron, K. S. & Sullivan, J. L. 1989. Severe herpesvirus infections in an adolescent without natural killer cells. *N Engl J Med,* 320**,** 1731-5.

Buchholz, V. R., Flossdorf, M., Hensel, I., Kretschmer, L., Weissbrich, B., Graf, P., Verschoor, A., Schiemann, M., Hofer, T. & Busch, D. H. 2013. Disparate individual fates compose robust CD8+ T cell immunity. *Science,* 340**,** 630-5.

Buchholz, V. R., Schumacher, T. N. M. & Busch, D. H. 2016. T Cell Fate at the Single-Cell Level. *Annual Review of Immunology,* 34**,** 65-92.

Burga, R. A., Thorn, M., Point, G. R., Guha, P., Nguyen, C. T., Licata, L. A., Dematteo, R. P., Ayala, A., Joseph Espat, N., Junghans, R. P. & Katz, S. C. 2015. Liver myeloid-derived suppressor cells expand in response to liver metastases in mice and inhibit the anti-tumor efficacy of anti-CEA CAR-T. *Cancer Immunol Immunother,* 64**,** 817-29.

Busch, D. H. & Pamer, E. G. 1999. T cell affinity maturation by selective expansion during infection. *J Exp Med,* 189**,** 701-10.

Busch, D. H., Pilip, I. & Pamer, E. G. 1998. Evolution of a complex T cell receptor repertoire during primary and recall bacterial infection. *J Exp Med,* 188**,** 61-70.

Cao, J., Packer, J. S., Ramani, V., Cusanovich, D. A., Huynh, C., Daza, R., Qiu, X., Lee, C., Furlan, S. N., Steemers, F. J., Adey, A., Waterston, R. H., Trapnell, C. & Shendure, J. 2017. Comprehensive single-cell transcriptional profiling of a multicellular organism. *Science,* 357**,** 661-667.

Cavazzana-Calvo, M., Payen, E., Negre, O., Wang, G., Hehir, K., Fusil, F., Down, J., Denaro, M., Brady, T., Westerman, K., Cavallesco, R., Gillet-Legrand, B., Caccavelli, L., Sgarra, R., Maouche-Chretien, L., Bernaudin, F., Girot, R., Dorazio, R., Mulder, G. J.,

Polack, A., Bank, A., Soulier, J., Larghero, J., Kabbara, N., Dalle, B., Gourmel, B., Socie, G., Chretien, S., Cartier, N., Aubourg, P., Fischer, A., Cornetta, K., Galacteros, F., Beuzard, Y., Gluckman, E., Bushman, F., Hacein-Bey-Abina, S. & Leboulch, P. 2010. Transfusion independence and HMGA2 activation after gene therapy of human beta-thalassaemia. *Nature,* 467**,** 318-22.

Chang, A. L., Miska, J., Wainwright, D. A., Dey, M., Rivetta, C. V., Yu, D., Kanojia, D., Pituch, K. C., Qiao, J., Pytel, P., Han, Y., Wu, M., Zhang, L., Horbinski, C. M., Ahmed, A. U. & Lesniak, M. S. 2016. CCL2 Produced by the Glioma Microenvironment Is Essential for the Recruitment of Regulatory T Cells and Myeloid-Derived Suppressor Cells. *Cancer Res,* 76**,** 5671-5682.

Chiu, D. K., Xu, I. M., Lai, R. K., Tse, A. P., Wei, L. L., Koh, H. Y., Li, L. L., Lee, D., Lo, R. C., Wong, C. M., Ng, I. O. & Wong, C. C. 2016. Hypoxia induces myeloid-derived suppressor cell recruitment to hepatocellular carcinoma through chemokine (C-C motif) ligand 26. *Hepatology,* 64**,** 797-813.

Chow, M. T., Ozga, A. J., Servis, R. L., Frederick, D. T., Lo, J. A., Fisher, D. E., Freeman, G. J., Boland, G. M. & Luster, A. D. 2019. Intratumoral Activity of the CXCR3 Chemokine System Is Required for the Efficacy of Anti-PD-1 Therapy. *Immunity,* 50**,** 1498-1512 e5.

Cohen, K. W., Linderman, S. L., Moodie, Z., Czartoski, J., Lai, L., Mantus, G., Norwood, C., Nyhoff, L. E., Edara, V. V., Floyd, K., De Rosa, S. C., Ahmed, H., Whaley, R., Patel, S. N., Prigmore, B., Lemos, M. P., Davis, C. W., Furth, S., O'keefe, J. B., Gharpure, M. P., Gunisetty, S., Stephens, K., Antia, R., Zarnitsyna, V. I., Stephens, D. S., Edupuganti, S., Rouphael, N., Anderson, E. J., Mehta, A. K., Wrammert, J., Suthar, M. S., Ahmed, R. & Mcelrath, M. J. 2021. Longitudinal analysis shows durable and broad immune memory after SARS-CoV-2 infection with persisting antibody responses and memory B and T cells. *Cell Rep Med,* 2**,** 100354.

Cook, D. N., Prosser, D. M., Forster, R., Zhang, J., Kuklin, N. A., Abbondanzo, S. J., Niu, X. D., Chen, S. C., Manfra, D. J., Wiekowski, M. T., Sullivan, L. M., Smith, S. R., Greenberg, H. B., Narula, S. K., Lipp, M. & Lira, S. A. 2000. CCR6 mediates dendritic cell localization, lymphocyte homeostasis, and immune responses in mucosal tissue. *Immunity,* 12**,** 495-503.

Curiel, T. J., Coukos, G., Zou, L., Alvarez, X., Cheng, P., Mottram, P., Evdemon-Hogan, M., Conejo-Garcia, J. R., Zhang, L., Burow, M., Zhu, Y., Wei, S., Kryczek, I., Daniel, B., Gordon, A., Myers, L., Lackner, A., Disis, M. L., Knutson, K. L., Chen, L. & Zou, W. 2004. Specific recruitment of regulatory T cells in ovarian carcinoma fosters immune privilege and predicts reduced survival. *Nat Med,* 10**,** 942-9.

Dai, L. & Gao, G. F. 2021. Viral targets for vaccines against COVID-19. *Nat Rev Immunol,* 21**,** 73-82.

De Kleer, I., Willems, F., Lambrecht, B. & Goriely, S. 2014. Ontogeny of myeloid cells. *Front Immunol,* 5**,** 423.

Di Pilato, M., Kfuri-Rubens, R., Pruessmann, J. N., Ozga, A. J., Messemaker, M., Cadilha, B. L., Sivakumar, R., Cianciaruso, C., Warner, R. D., Marangoni, F., Carrizosa, E., Lesch, S., Billingsley, J., Perez-Ramos, D., Zavala, F., Rheinbay, E., Luster, A. D., Gerner, M. Y., Kobold, S., Pittet, M. J. & Mempel, T. R. 2021. CXCR6 positions cytotoxic T cells to receive critical survival signals in the tumor microenvironment. *Cell,* 184**,** 4512-4530 e22.

Bibliography

Dokun, A. O., Kim, S., Smith, H. R. C., Kang, H.-S. P., Chu, D. T. & Yokoyama, W. M. 2001. Specific and nonspecific NK cell activation during virus infection. *Nature Immunology,* 2**,** 951-956.

Doudna, J. A. & Charpentier, E. 2014. Genome editing. The new frontier of genome engineering with CRISPR-Cas9. *Science,* 346**,** 1258096.

Eraslan, G., Avsec, Z., Gagneur, J. & Theis, F. J. 2019. Deep learning: new computational modelling techniques for genomics. *Nat Rev Genet,* 20**,** 389-403.

Fan, H. C., Fu, G. K. & Fodor, S. P. 2015. Expression profiling. Combinatorial labeling of single cells for gene expression cytometry. *Science,* 347**,** 1258367.

Gambotto, A., Dworacki, G., Cicinnati, V., Kenniston, T., Steitz, J., Tuting, T., Robbins, P. D. & Deleo, A. B. 2000. Immunogenicity of enhanced green fluorescent protein (EGFP) in BALB/c mice: identification of an H2-Kd-restricted CTL epitope. *Gene Ther,* 7**,** 2036-40.

Gerlach, C., Rohr, J. C., Perie, L., Van Rooij, N., Van Heijst, J. W., Velds, A., Urbanus, J., Naik, S. H., Jacobs, H., Beltman, J. B., De Boer, R. J. & Schumacher, T. N. 2013. Heterogeneous differentiation patterns of individual CD8+ T cells. *Science,* 340**,** 635-9.

Glanzmann, E. & Riniker, P. 1950. [Essential lymphocytophthisis; new clinical aspect of infant pathology]. *Ann Paediatr,* 175**,** 1-32.

Grassmann, S., Pachmayr, L. O., Leube, J., Mihatsch, L., Andrae, I., Flommersfeld, S., Oduro, J., Cicin-Sain, L., Schiemann, M., Flossdorf, M. & Buchholz, V. R. 2019. Distinct Surface Expression of Activating Receptor Ly49H Drives Differential Expansion of NK Cell Clones upon Murine Cytomegalovirus Infection. *Immunity,* 50**,** 1391-1400 e4.

Griffith, J. W., Sokol, C. L. & Luster, A. D. 2014. Chemokines and chemokine receptors: positioning cells for host defense and immunity. *Annu Rev Immunol,* 32**,** 659-702.

Hacein-Bey-Abina, S., Von Kalle, C., Schmidt, M., Mccormack, M. P., Wulffraat, N., Leboulch, P., Lim, A., Osborne, C. S., Pawliuk, R., Morillon, E., Sorensen, R., Forster, A., Fraser, P., Cohen, J. I., De Saint Basile, G., Alexander, I., Wintergerst, U., Frebourg, T., Aurias, A., Stoppa-Lyonnet, D., Romana, S., Radford-Weiss, I., Gross, F., Valensi, F., Delabesse, E., Macintyre, E., Sigaux, F., Soulier, J., Leiva, L. E., Wissler, M., Prinz, C., Rabbitts, T. H., Le Deist, F., Fischer, A. & Cavazzana-Calvo, M. 2003. LMO2-associated clonal T cell proliferation in two patients after gene therapy for SCID-X1. *Science,* 302**,** 415-9.

Hammer, Q., Rückert, T., Borst, E. M., Dunst, J., Haubner, A., Durek, P., Heinrich, F., Gasparoni, G., Babic, M., Tomic, A., Pietra, G., Nienen, M., Blau, I. W., Hofmann, J., Na, I. K., Prinz, I., Koenecke, C., Hemmati, P., Babel, N., Arnold, R., Walter, J., Thurley, K., Mashreghi, M. F., Messerle, M. & Romagnani, C. 2018. Peptide-specific recognition of human cytomegalovirus strains controls adaptive natural killer cells. *Nat Immunol,* 19**,** 453-463.

Heslop, H. E., Slobod, K. S., Pule, M. A., Hale, G. A., Rousseau, A., Smith, C. A., Bollard, C. M., Liu, H., Wu, M. F., Rochester, R. J., Amrolia, P. J., Hurwitz, J. L., Brenner, M. K. & Rooney, C. M. 2010. Long-term outcome of EBV-specific T-cell infusions to prevent or treat EBV-related lymphoproliferative disease in transplant recipients. *Blood,* 115**,** 925-35.

Hilleman, M. R., Weibel, R. E., Buynak, E. B., Stokes, J., Jr. & Whitman, J. E., Jr. 1967. Live attenuated mumps-virus vaccine. IV. Protective efficacy as measured in a field evaluation. *N Engl J Med,* 276**,** 252-8.

Hodi, F. S., O'day, S. J., Mcdermott, D. F., Weber, R. W., Sosman, J. A., Haanen, J. B., Gonzalez, R., Robert, C., Schadendorf, D., Hassel, J. C., Akerley, W., Van Den Eertwegh, A. J., Lutzky, J., Lorigan, P., Vaubel, J. M., Linette, G. P., Hogg, D., Ottensmeier, C. H., Lebbe, C., Peschel, C., Quirt, I., Clark, J. I., Wolchok, J. D., Weber, J. S., Tian, J., Yellin, M. J., Nichol, G. M., Hoos, A. & Urba, W. J. 2010. Improved survival with ipilimumab in patients with metastatic melanoma. *N Engl J Med,* 363**,** 711-23.

Holst, J., Szymczak-Workman, A. L., Vignali, K. M., Burton, A. R., Workman, C. J. & Vignali, D. A. A. 2006. Generation of T-cell receptor retrogenic mice. *Nature Protocols,* 1**,** 406.

Iellem, A., Mariani, M., Lang, R., Recalde, H., Panina-Bordignon, P., Sinigaglia, F. & D'ambrosio, D. 2001. Unique chemotactic response profile and specific expression of chemokine receptors CCR4 and CCR8 by CD4(+)CD25(+) regulatory T cells. *J Exp Med,* 194**,** 847-53.

Jagannathan-Bogdan, M. & Zon, L. I. 2013. Hematopoiesis. *Development,* 140**,** 2463-7.

Jameson, S. C. 2002. Maintaining the norm: T-cell homeostasis. *Nat Rev Immunol,* 2**,** 547-56.

Jenner, E. 1801. On the Origin of the Vaccine Inoculation. *Med Phys J,* 5**,** 505-508.

Jovic, D., Liang, X., Zeng, H., Lin, L., Xu, F. & Luo, Y. 2022. Single-cell RNA sequencing technologies and applications: A brief overview. *Clin Transl Med,* 12**,** e694.

Kim, S., Iizuka, K., Kang, H. S., Dokun, A., French, A. R., Greco, S. & Yokoyama, W. M. 2002. In vivo developmental stages in murine natural killer cell maturation. *Nat Immunol,* 3**,** 523-8.

Kim, S., Poursine-Laurent, J., Truscott, S. M., Lybarger, L., Song, Y. J., Yang, L., French, A. R., Sunwoo, J. B., Lemieux, S., Hansen, T. H. & Yokoyama, W. M. 2005. Licensing of natural killer cells by host major histocompatibility complex class I molecules. *Nature,* 436**,** 709-13.

Kishihara, K., Penninger, J., Wallace, V. A., Kundig, T. M., Kawai, K., Wakeham, A., Timms, E., Pfeffer, K., Ohashi, P. S., Thomas, M. L. & Et Al. 1993. Normal B lymphocyte development but impaired T cell maturation in CD45-exon6 protein tyrosine phosphatase-deficient mice. *Cell,* 74**,** 143-56.

Koch, U. & Radtke, F. 2011. Mechanisms of T cell development and transformation. *Annu Rev Cell Dev Biol,* 27**,** 539-62.

Kondo, M., Weissman, I. L. & Akashi, K. 1997. Identification of clonogenic common lymphoid progenitors in mouse bone marrow. *Cell,* 91**,** 661-72.

Kurth, I., Willimann, K., Schaerli, P., Hunziker, T., Clark-Lewis, I. & Moser, B. 2001. Monocyte selectivity and tissue localization suggests a role for breast and kidney-expressed chemokine (BRAK) in macrophage development. *J Exp Med,* 194**,** 855-61.

Lesch, S., Blumenberg, V., Stoiber, S., Gottschlich, A., Ogonek, J., Cadilha, B. L., Dantes, Z., Rataj, F., Dorman, K., Lutz, J., Karches, C. H., Heise, C., Kurzay, M., Larimer, B. M., Grassmann, S., Rapp, M., Nottebrock, A., Kruger, S., Tokarew, N., Metzger, P., Hoerth, C., Benmebarek, M. R., Dhoqina, D., Grunmeier, R., Seifert, M., Oener, A., Umut, O., Joaquina, S., Vimeux, L., Tran, T., Hank, T., Baba, T., Huynh, D., Megens, R. T. A., Janssen, K. P., Jastroch, M., Lamp, D., Ruehland, S., Di Pilato, M., Pruessmann, J. N.,

Thomas, M., Marr, C., Ormanns, S., Reischer, A., Hristov, M., Tartour, E., Donnadieu, E., Rothenfusser, S., Duewell, P., Konig, L. M., Schnurr, M., Subklewe, M., Liss, A. S., Halama, N., Reichert, M., Mempel, T. R., Endres, S. & Kobold, S. 2021. T cells armed with C-X-C chemokine receptor type 6 enhance adoptive cell therapy for pancreatic tumours. *Nat Biomed Eng,* 5**,** 1246-1260.

Li, Z., Dullmann, J., Schiedlmeier, B., Schmidt, M., Von Kalle, C., Meyer, J., Forster, M., Stocking, C., Wahlers, A., Frank, O., Ostertag, W., Kuhlcke, K., Eckert, H. G., Fehse, B. & Baum, C. 2002. Murine leukemia induced by retroviral gene marking. *Science,* 296**,** 497.

Love, P. E. & Bhandoola, A. 2011. Signal integration and crosstalk during thymocyte migration and emigration. *Nat Rev Immunol,* 11**,** 469-77.

Lu, P., Youngblood, B. A., Austin, J. W., Mohammed, A. U., Butler, R., Ahmed, R. & Boss, J. M. 2014. Blimp-1 represses CD8 T cell expression of PD-1 using a feed-forward transcriptional circuit during acute viral infection. *J Exp Med,* 211**,** 515-27.

Luther, S. A., Ansel, K. M. & Cyster, J. G. 2003. Overlapping roles of CXCL13, interleukin 7 receptor alpha, and CCR7 ligands in lymph node development. *J Exp Med,* 197**,** 1191-8.

Male, V., Nisoli, I., Kostrzewski, T., Allan, D. S., Carlyle, J. R., Lord, G. M., Wack, A. & Brady, H. J. 2014. The transcription factor E4bp4/Nfil3 controls commitment to the NK lineage and directly regulates Eomes and Id2 expression. *J Exp Med,* 211**,** 635-42.

Maude, S. L., Laetsch, T. W., Buechner, J., Rives, S., Boyer, M., Bittencourt, H., Bader, P., Verneris, M. R., Stefanski, H. E., Myers, G. D., Qayed, M., De Moerloose, B., Hiramatsu, H., Schlis, K., Davis, K. L., Martin, P. L., Nemecek, E. R., Yanik, G. A., Peters, C., Baruchel, A., Boissel, N., Mechinaud, F., Balduzzi, A., Krueger, J., June, C. H., Levine, B. L., Wood, P., Taran, T., Leung, M., Mueller, K. T., Zhang, Y., Sen, K., Lebwohl, D., Pulsipher, M. A. & Grupp, S. A. 2018. Tisagenlecleucel in Children and Young Adults with B-Cell Lymphoblastic Leukemia. *N Engl J Med,* 378**,** 439-448.

Mercier, F. E., Ragu, C. & Scadden, D. T. 2011. The bone marrow at the crossroads of blood and immunity. *Nat Rev Immunol,* 12**,** 49-60.

Mitchell, R. S., Beitzel, B. F., Schroder, A. R., Shinn, P., Chen, H., Berry, C. C., Ecker, J. R. & Bushman, F. D. 2004. Retroviral DNA integration: ASLV, HIV, and MLV show distinct target site preferences. *PLoS Biol,* 2**,** E234.

Moon, E. K., Carpenito, C., Sun, J., Wang, L. C., Kapoor, V., Predina, J., Powell, D. J., Jr., Riley, J. L., June, C. H. & Albelda, S. M. 2011. Expression of a functional CCR2 receptor enhances tumor localization and tumor eradication by retargeted human T cells expressing a mesothelin-specific chimeric antibody receptor. *Clin Cancer Res,* 17**,** 4719-30.

Nabekura, T. & Lanier, L. L. 2016. Activating Receptors for Self-MHC Class I Enhance Effector Functions and Memory Differentiation of NK Cells during Mouse Cytomegalovirus Infection. *Immunity,* 45**,** 74-82.

Naik, S. H., Perie, L., Swart, E., Gerlach, C., Van Rooij, N., De Boer, R. J. & Schumacher, T. N. 2013. Diverse and heritable lineage imprinting of early haematopoietic progenitors. *Nature,* 496**,** 229-32.

Neelapu, S. S., Locke, F. L., Bartlett, N. L., Lekakis, L. J., Miklos, D. B., Jacobson, C. A., Braunschweig, I., Oluwole, O. O., Siddiqi, T., Lin, Y., Timmerman, J. M., Stiff, P. J., Friedberg, J. W., Flinn, I. W., Goy, A., Hill, B. T., Smith, M. R., Deol, A., Farooq, U.,

Mcsweeney, P., Munoz, J., Avivi, I., Castro, J. E., Westin, J. R., Chavez, J. C., Ghobadi, A., Komanduri, K. V., Levy, R., Jacobsen, E. D., Witzig, T. E., Reagan, P., Bot, A., Rossi, J., Navale, L., Jiang, Y., Aycock, J., Elias, M., Chang, D., Wiezorek, J. & Go, W. Y. 2017. Axicabtagene Ciloleucel CAR T-Cell Therapy in Refractory Large B-Cell Lymphoma. *N Engl J Med,* 377**,** 2531-2544.

Newby, G. A., Yen, J. S., Woodard, K. J., Mayuranathan, T., Lazzarotto, C. R., Li, Y., Sheppard-Tillman, H., Porter, S. N., Yao, Y., Mayberry, K., Everette, K. A., Jang, Y., Podracky, C. J., Thaman, E., Lechauve, C., Sharma, A., Henderson, J. M., Richter, M. F., Zhao, K. T., Miller, S. M., Wang, T., Koblan, L. W., Mccaffrey, A. P., Tisdale, J. F., Kalfa, T. A., Pruett-Miller, S. M., Tsai, S. Q., Weiss, M. J. & Liu, D. R. 2021. Base editing of haematopoietic stem cells rescues sickle cell disease in mice. *Nature,* 595**,** 295-302.

Ohl, L., Henning, G., Krautwald, S., Lipp, M., Hardtke, S., Bernhardt, G., Pabst, O. & Forster, R. 2003. Cooperating mechanisms of CXCR5 and CCR7 in development and organization of secondary lymphoid organs. *J Exp Med,* 197**,** 1199-204.

Orr, M. T., Murphy, W. J. & Lanier, L. L. 2010. 'Unlicensed' natural killer cells dominate the response to cytomegalovirus infection. *Nat Immunol,* 11**,** 321-7.

Pachmayr, L. O., Muehlbauer, A., Flommersfeld, S., Graml, F., Hoenninger, J., Von Baumgarten, L., Buchholz, V. R. & Grassmann, S. 2023. Unbiased chemokine receptor screening reveals similar efficacy of lymph node- and tumor-targeted T cell immunotherapy. *Cancer Immunol Immunother,* 72**,** 3111-3124.

Papalexi, E. & Satija, R. 2018. Single-cell RNA sequencing to explore immune cell heterogeneity. *Nat Rev Immunol,* 18**,** 35-45.

Pasteur, M. L. 1881a. On Chicken Cholera: Study of the Conditions of Non-Recidivation and of Some Other Characteristics of This Disease. *Science,* 2**,** 126-7.

Pasteur, M. L. 1881b. On Chicken Cholera: Study of the Conditions of Non-Recidivation and of Some Other Characteristics of This Disease. *Science,* 2**,** 55-7.

Peled, A., Petit, I., Kollet, O., Magid, M., Ponomaryov, T., Byk, T., Nagler, A., Ben-Hur, H., Many, A., Shultz, L., Lider, O., Alon, R., Zipori, D. & Lapidot, T. 1999. Dependence of human stem cell engraftment and repopulation of NOD/SCID mice on CXCR4. *Science,* 283**,** 845-8.

Peng, W., Ye, Y., Rabinovich, B. A., Liu, C., Lou, Y., Zhang, M., Whittington, M., Yang, Y., Overwijk, W. W., Lizee, G. & Hwu, P. 2010. Transduction of tumor-specific T cells with CXCR2 chemokine receptor improves migration to tumor and antitumor immune responses. *Clin Cancer Res,* 16**,** 5458-68.

Polack, F. P., Thomas, S. J., Kitchin, N., Absalon, J., Gurtman, A., Lockhart, S., Perez, J. L., Perez Marc, G., Moreira, E. D., Zerbini, C., Bailey, R., Swanson, K. A., Roychoudhury, S., Koury, K., Li, P., Kalina, W. V., Cooper, D., Frenck, R. W., Jr., Hammitt, L. L., Tureci, O., Nell, H., Schaefer, A., Unal, S., Tresnan, D. B., Mather, S., Dormitzer, P. R., Sahin, U., Jansen, K. U., Gruber, W. C. & Group, C. C. T. 2020. Safety and Efficacy of the BNT162b2 mRNA Covid-19 Vaccine. *N Engl J Med,* 383**,** 2603-2615.

Ranzani, M., Cesana, D., Bartholomae, C. C., Sanvito, F., Pala, M., Benedicenti, F., Gallina, P., Sergi, L. S., Merella, S., Bulfone, A., Doglioni, C., Von Kalle, C., Kim, Y. J., Schmidt, M., Tonon, G., Naldini, L. & Montini, E. 2013. Lentiviral vector-based insertional mutagenesis identifies genes associated with liver cancer. *Nat Methods,* 10**,** 155-61.

Rapp, M., Grassmann, S., Chaloupka, M., Layritz, P., Kruger, S., Ormanns, S., Rataj, F., Janssen, K. P., Endres, S., Anz, D. & Kobold, S. 2016. C-C chemokine receptor type-4 transduction of T cells enhances interaction with dendritic cells, tumor infiltration and therapeutic efficacy of adoptive T cell transfer. *Oncoimmunology,* 5**,** e1105428.

Reif, A. E. & Allen, J. M. 1964. The Akr Thymic Antigen and Its Distribution in Leukemias and Nervous Tissues. *J Exp Med,* 120**,** 413-33.

Rosenberg, S. A., Yang, J. C., Sherry, R. M., Kammula, U. S., Hughes, M. S., Phan, G. Q., Citrin, D. E., Restifo, N. P., Robbins, P. F., Wunderlich, J. R., Morton, K. E., Laurencot, C. M., Steinberg, S. M., White, D. E. & Dudley, M. E. 2011. Durable complete responses in heavily pretreated patients with metastatic melanoma using T-cell transfer immunotherapy. *Clin Cancer Res,* 17**,** 4550-7.

Rückert, T., Lareau, C. A., Mashreghi, M. F., Ludwig, L. S. & Romagnani, C. 2022. Clonal expansion and epigenetic inheritance of long-lasting NK cell memory. *Nat Immunol,* 23**,** 1551-1563.

Rupp, L. J., Schumann, K., Roybal, K. T., Gate, R. E., Ye, C. J., Lim, W. A. & Marson, A. 2017. CRISPR/Cas9-mediated PD-1 disruption enhances anti-tumor efficacy of human chimeric antigen receptor T cells. *Sci Rep,* 7**,** 737.

Sallusto, F., Geginat, J. & Lanzavecchia, A. 2004. Central memory and effector memory T cell subsets: function, generation, and maintenance. *Annu Rev Immunol,* 22**,** 745-63.

Sather, B. D., Treuting, P., Perdue, N., Miazgowicz, M., Fontenot, J. D., Rudensky, A. Y. & Campbell, D. J. 2007. Altering the distribution of Foxp3(+) regulatory T cells results in tissue-specific inflammatory disease. *J Exp Med,* 204**,** 1335-47.

Schepers, K., Swart, E., Van Heijst, J. W., Gerlach, C., Castrucci, M., Sie, D., Heimerikx, M., Velds, A., Kerkhoven, R. M., Arens, R. & Schumacher, T. N. 2008. Dissecting T cell lineage relationships by cellular barcoding. *J Exp Med,* 205**,** 2309-18.

Schlecker, E., Stojanovic, A., Eisen, C., Quack, C., Falk, C. S., Umansky, V. & Cerwenka, A. 2012. Tumor-infiltrating monocytic myeloid-derived suppressor cells mediate CCR5-dependent recruitment of regulatory T cells favoring tumor growth. *J Immunol,* 189**,** 5602-11.

Shen, F. W., Saga, Y., Litman, G., Freeman, G., Tung, J. S., Cantor, H. & Boyse, E. A. 1985. Cloning of Ly-5 cDNA. *Proc Natl Acad Sci U S A,* 82**,** 7360-3.

Skelton, D., Satake, N. & Kohn, D. B. 2001. The enhanced green fluorescent protein (eGFP) is minimally immunogenic in C57BL/6 mice. *Gene Ther,* 8**,** 1813-4.

Stemberger, C., Huster, K. M., Koffler, M., Anderl, F., Schiemann, M., Wagner, H. & Busch, D. H. 2007. A single naive CD8+ T cell precursor can develop into diverse effector and memory subsets. *Immunity,* 27**,** 985-97.

Stripecke, R., Carmen Villacres, M., Skelton, D., Satake, N., Halene, S. & Kohn, D. 1999. Immune response to green fluorescent protein: implications for gene therapy. *Gene Ther,* 6**,** 1305-12.

Sun, J. C., Beilke, J. N. & Lanier, L. L. 2009. Adaptive immune features of natural killer cells. *Nature,* 457**,** 557-61.

Sun, J. C. & Lanier, L. L. 2011. NK cell development, homeostasis and function: parallels with CD8(+) T cells. *Nat Rev Immunol,* 11**,** 645-57.

Bibliography

Tsui, C., Kretschmer, L., Rapelius, S., Gabriel, S. S., Chisanga, D., Knopper, K., Utzschneider, D. T., Nussing, S., Liao, Y., Mason, T., Torres, S. V., Wilcox, S. A., Kanev, K., Jarosch, S., Leube, J., Nutt, S. L., Zehn, D., Parish, I. A., Kastenmuller, W., Shi, W., Buchholz, V. R. & Kallies, A. 2022. MYB orchestrates T cell exhaustion and response to checkpoint inhibition. *Nature,* 609**,** 354-360.

Vickovic, S., Eraslan, G., Salmén, F., Klughammer, J., Stenbeck, L., Schapiro, D., Äijö, T., Bonneau, R., Bergenstråhle, L., Navarro, J. F., Gould, J., Griffin, G. K., Borg, Å., Ronaghi, M., Frisén, J., Lundeberg, J., Regev, A. & Ståhl, P. L. 2019. High-definition spatial transcriptomics for in situ tissue profiling. *Nature Methods,* 16**,** 987-990.

Williams, D. A. 1994. Molecular analysis of the hematopoietic microenvironment. *Pediatr Res,* 36**,** 557-60.

Wu, N., Joyal-Desmarais, K., Ribeiro, P. A. B., Vieira, A. M., Stojanovic, J., Sanuade, C., Yip, D. & Bacon, S. L. 2023. Long-term effectiveness of COVID-19 vaccines against infections, hospitalisations, and mortality in adults: findings from a rapid living systematic evidence synthesis and meta-analysis up to December, 2022. *Lancet Respir Med,* 11**,** 439-452.

7 Acknowledgements

The completion of this thesis relied on the continuous support from many important people to whom I am deeply grateful.

I would like to thank my supervisors Veit Buchholz and Dirk Busch for their support and guidance throughout my research, contributing greatly to the success of this work with profound scientific discussions and valuable suggestions, while providing a cherishable work environment at the technical state of the art, all within the doctoral program *Translational Medicine*.

Particularly, I want to express my deep gratitude to my direct supervisor and teacher Simon Grassmann, who taught me my skillset both technically as well as conceptually, supported me at any time during my thesis, and still is a dear mentor and friend within as well as outside of research.

Numerous colleagues and collaborators critically contributed to this thesis and my time at the institute. Among these, I would like to offer my special thanks to Sophie Jarosch, Immanuel Andrä, Anton Mühlbauer, Sebastian Jarosch, Inge Hensel, Monika Hammel and Franziska Graml, who made my time at the institute a joyful experience. Furthermore, Matthias Schiemann and his group set up the Flow Cytometry Core Facility (CyTUM), which was indispensable for my work. Discussions with Joseph Sun and Lewis Lanier apart from the institute helped to put my findings into context and were thus deeply appreciated. Michael Kirstein, representing the whole team of veterinarians and animal care-takers at the institute, enabled a professional and thus deeply appreciated work with experimental animals. At this point, I want to express my sincere respect towards all animals that are part of ethically justified experiments, contributing profoundly to advance in numerous areas of research, as this was the case in my thesis as well.

Not to forget, I am deeply grateful for the unwavering support of my family and friends. In particular, I would like to thank my parents Elisabeth and Otto, as well as my brother and sisters, Maximilian, Ursula and Eva. Furthermore, I would like to mention Maximilian and Severin, my friends and former co-tenants, whom I owe valuable guidance amongst my studies and thesis as well as unforgettable years as roommates.

At long last, I want to thank my dear wife Isabelle for believing in me at any time and supporting me in any aspect.